99-207

Environment Canada / Environnement Canada

Canada

BASELINE PHYSICAL LIMNOLOGY OF THE UPPER ARROW LAKES RESERVOIR

P.F. Hamblin

NWRI Contribution Number 99-207

NAL WATER
H INSTITUTE
NATIONAL DE
E SUR LES EAUX

Baseline Physical Limnology of the Upper Arrow Lakes Reservoir

By

Paul F. Hamblin
Aquatic Ecosystem Restoration Branch
National Water Research Institute

NWRI Cont. #99-207

National Water Research Institute Contribution

December, 1998

1

MANAGEMENT PERSPECTIVE

At the request of the B.C. Ministry of Environment this observational study of the circulation regime of the Arrow Lakes was undertaken to assist in the assessment and optimization of a strategy for the artificial fertilization of the reservoir. The biodiversity of the lake is at risk with the sudden decline of the kokanee sports fishery.

This document reports on the temperature and flows at critical areas in the system that could be surveyed within the limitations of the instrumentation. The results could form the basis for future lake remediation employing nutrient addition.

These results will be disseminated to the appropriate persons making the decisions on how best to mitigate the collapse of the Arrow Lakes sports fishery.

PERSPECTIVE DE GESTION

À la demande du Ministère de l'environnement de la Colombie-Britannique, l'observation du régime de la circulation dans les lacs Arrow a été entreprise afin d'aider à évaluer et à optimiser une stratégie de fertilisation artificielle du réservoir. La baisse soudaine de la pêche sportive du saumon kokani met en danger la biodiversité du lac.

Ce document rend compte de la température et des débits dans les zones critiques du réseau hydrographique que les capacités limitées des instruments ont permis de relever. Les résultats pourraient servir de point de départ à d'autres rétablissements de lacs par addition de substances nutritives.

Ces résultats seront distribués aux personnes qui décideront de la meilleure façon d'atténuer l'effondrement de la pêche sportive dans les lacs Arrow.

ABSTRACT

Field observations of temperature and current profiles were taken during August 1997 in the Upper Arrow Lakes Reservoir for the purposes of determining the baseline limnology in the event that lake fertization would be undertaken to restore the declining kokanee sports fishery. Highlights and analyses of these observations are provided in this report.

Most of the effort was devoted to studying the exchange between the Upper and Lower Lakes and the pattern of flow in the inflow region of the lake. In both cases the circulation was found to be complex and due to the water stratification, bathymetry and the earth's rotation. Implications are given for the addition of nutrients. At the same time some novel instrumentation were evaluated in this ultra oligotrophic lake.

RÉSUMÉ

Les observations sur le terrain de profils de température et de courant ont été effectuées en août 1997, dans le réservoir du lac Upper Arrow, pour déterminer la limnologie de base au cas où la fertilisation du lac serait entreprise afin de rétablir la pêche sportive du saumon kokani en déclin. Des points saillants et des analyses de ces observations sont fournis dans ce rapport.

Les efforts ont principalement été consacrés à l'étude des échanges entre les lacs Upper et Lower et à la configuration de l'écoulement dans la zone de débit entrant des lacs. Dans les deux cas, on a trouvé que la stratification de l'eau, la bathymétrie et la rotation de la Terre engendrent une circulation complexe. Les conséquences liées à l'ajout de substances nutritives sont indiquées. Au cours de ces observations, de nouveaux instruments ont été évalués dans ces lacs très oligotrophes.

1. Introduction

The British Columbia Ministry of Environment, Lands and Parks (MELP) has identified a need for the baseline limnology of the Arrow Lakes Reservoir which has been stimulated by rapid ecological changes in the system as evidenced by the sudden decline of the Kokanee sports fishery. Before a programme of lake fertilization can be initiated as has been successfully undertaken in the nearby, Kootenay Lake, (Ashley et al., 1997, Rae et al.,1996), it is desirable to assess the likelihood of success. This necessitates some understanding of limnology of the reservoir system. As one component of the study, currents and water temperatures were measured during the period from August 19 to August 28, 1997. This report is intended to provide some displays and analyses of those field observations taken in the Upper Arrow Lakes Reservoir. The reader is referred to a similar report on the Lower Arrow Lakes Reservoir (Hamblin, 1998).

In a study undertaken in order to provide an assessment of the likely alteration to the thermal regime from a proposed development of a hydroelectric generating station at a dam located at the outlet of the Lower Lake (Hamblin, 1997) some initial water quality modelling was undertaken which focused on the thermal and total dissolved thermal regimes. Hamblin identified the need for improved knowledge of the exchange of water between the two lakes and for knowledge of the bathymetry of the two lake basins in electronic form so that more accurate numerical modelling could be performed. Part of this report deals with the reduction of recently purchased digital bathymetry into forms suitable for vertical one and two-dimensional modelling and for three-dimensional modelling.

Currents were measured in this survey by means of an underway acoustic doppler profiler (ADCP). Despite the high frequency of this device (1200 KHz) there was concern that the lack of suspended particles which act as scatterers of the acoustic signal would render the meter inoperable. Evidently Secchi depths as high as 26m have been observed in this ultra oligotrophic lake. Part of the report is devoted to an evaluation of the performance of the broadband ADCP in this unusual environment. A similar instrument was operated successfully in Kootenay Lake in 1993 (Hamblin et al.,1995) but only after the study area had been fertilized sufficiently to build up the concentration of scatterers. Because of the known interaction of flow and density stratification attempts were made to simultaneously sample current and temperature. As well, in a previous study of the distribution of temperature and dissolved solids of the Arrow Lakes Reservoir, Hamblin and McAdam (1997) found that an autonomous Global Positioning System (GPS) worked erratically with frequent large errors in horizontal location that had to be resolved with reference to an echo sounder and bathymetric charts. Further attention is given to an assessment of a base-station differential GPS which was integrated directly into the recording system of the ADCP. Recommendations are made on the future use of the new technology used in this study.

2. Bathymetric and Hypsographic Analyses

As input of basin geometry for such one-dimensional water quality models as DYRESM (Hamblin, 1997), area and volume distributions as a function of depth or distance above the bottom must be specified. Furthermore, three-dimensional transport and circulation models require basin geometry at model mesh points. For example, the automated mesh generator, TRIGRID, requires as input the lake's shoreline configuration as a continuous sequence of positions in a clockwise sense around the perimeter of the lake. While the input of deeper topography can be either in continuous contour or random form, continuous bathymetric contours are particularly convenient for the calculation of the area enclosed by a given contour.

As a first step, the Canadian Hydrographic Service (CHS) chart of the Upper Arrow Lakes, 3057 was purchased in electronic format from Nautical Data International. These data proved to be extremely difficult to process as all features such as the land and map features were included. The CHS staff at the Canada Centre for Inland Waters kindly reduced these data to two files per depth contour and chart, one for the forward side and the other for the back side of each chart with specialized software in their possession. In the case of chart 3057 there are three insets for the lake, each having an offset in position. A composite file was constructed for each contour of a given lake basin by concatenation of these individual files, but unlike the case of CHS chart 3056 for the Lower Lake allowance had to be made for these offsets. Unfortunately, not all the Upper Lake is contained on chart 3057. Some of the shoreline extends to 3058. This lack of data resulted in an underestimation of the surface area of the Upper Arrow Lake when compared to the surface area used by B.C. Hydro. As the portion of the lake covered in chart 3058 is shallow this did not effect the estimation of the areas of deeper contours.

Next, a computer program was written to identify as many 320 individual arcs for a given contour, convert the geographic coordinates to eastings and northings in metres according to a Universal Transverse Mercator projection and plot the arc numbers. Unfortunately, the three overlapping map sections inserted duplicate arc numbers which could not be distinguished from one another on the plot. A routine had to be written to detect duplicate arcs and plot only one arc when a duplication occurred. The sequence of continuous arcs was then noted manually and fed into another program that plotted the position of every 10^{th} point both as a dot and also as a curve joining adjacent points. In this way missing arcs were identified as well as arcs reversed in direction. Finally, the positions at the junction from one arc to another were visually examined as a final stage of error checking. Sometimes, partially overlapping arcs were identified and eliminated in this way. To give an idea of the resolution of the contour data, in the case of the shoreline contour there are 35,099 points which are separated on average by a distance of 8.2m and a maximum separation of 1146m like due to a missing arc. Any gaps in the contours are assumed to be joined by straight lines.

Plots of the shoreline, 10m, 50m,100m and 200m depth contours are shown in Figures 1 to 5. The 2m depth contour was not processed in the interest of time and was considered to be little different from the shoreline contour. It is noteworthy that the 50m and 100m depth contours are divided into two separately closed contours. The area bounded by each contour was calculated from Green's theorem,

$Area = \frac{1}{2}\oint_c x\,\partial y - y\,\partial x$. The surface area obtained from the above expression is 282.2 Km^2 which is considerably less than that used by BC Hydro of 306 Km^2. The larger value was used in the calculation of volume. This is due to the portion of the Upper Lake on chart 3058 which was not available for the analysis. Once the area was known, the volume was calculated from the expression; $Volume = \int_0^{Sfc} area(z)\,\partial z$. Plots of the area and volume curves with depth are shown in Figure 6 based on the data tabulated in Table 1.

Depth (m)	Area (Km^2)	Volume (Km^3)
287	0	0
200	65.08	2.83
100	115.45	11.86
50	155.16	18.62
10	218.31	26.091
0	306 (282.2)	28.71

Table 1. Hypsographic Data, Upper Arrow Lake. The surface area based on CHS chart 3057 is in parentheses.

The area-depth curves of four intermontane lakes in British Columbia and the Yukon Ter. were compared in Hamblin (1997). It is seen that the curve in Figure 6 differs from that of Kootenay Lake (Hamblin, 1997). Since in the modelling exercise (Hamblin, 1997) the hypsographic curves were unknown, it was assumed that the Kootenay Lake data applied to the Arrow Lakes which is now seen to be not true for the Arrow Lakes. The difference in shape of the curves for the two lakes is due to the Narrows region which has a substantial contribution to the area of depths shallower than 50m in the case of the Arrow Lakes.

When the total volume is compared to that estimated by Hamblin (1997) based on the assumed Kootenay Lake hypsographic data and the extrema in the annual discharge curve it is seen that the former estimate is four times too large, due in part to the different distribution of volume in Kootenay Lake. Thus, the previous maximum and minimum residence times were estimated to be 83 and 21 months respectively. The correct times for the Upper Arrow Lakes Reservoir are now 20 and 5 months respectively.

3. Evaluation of the Navigation System

In Hamblin (1998) ship velocities calculated with differential GPS data were compared to acoustically derived bottom tracked velocities, with the result that acoustically determined reference velocities are still far more accurate compared to the electronic navigation method despite improvements with the differential system. As a further test of the new base-station differential GPS system positions are compared to those inferred from acoustic tracking. In the Narrows region ship tracks for the first four field experiments were estimated from bottom tracked velocities by integrating the east and north component equations relating velocity to position. The bottom tracks started from an arbitrary origin. These tracks are compared to direct track locations from the differential GPS in Figure 7 which shows that bottom tracked positions slowly migrate upstream with an apparent speed of up to 20.3 cm/s. Crossings from south to north compare more closely with the differential GPS positions than those from north to south. The manufacturer was consulted about these position differences and the explanation given was that they are due to small compass errors which accumulate along the track. These errors in position result in much smaller velocity errors. For example, a five degree compass error at the usual speed of the survey vessel would result in a 20cm/s speed error but the compass error also applies to the total flow measured by the doppler shifts. Since the vessel's velocity must be subtracted from the total flow, the flow error would be reduced to one cm/s for a flow speed of 20 cm/s. To assess whether these compass errors in bottom tracking influenced the transport calculations transport was calculated based on the average of the two south-to-north crossings of August 21 and compared to a similar calculation for the two north-to south transects. The transport for the south-to-north case was only 2.9% higher and the north-to south transect 6.4% lower than the overall average. Because the experiments were always composed of at least two opposite crossings the compass errors should nearly cancel one another and contribute little to the overall error.

Since the track plots suggests that reference velocity based on differential GPS ought to be more stable than bottom tracking the raw data for the August 21 case was reprocessed using the playback module of TRANSECT, the field data gathering software supplied by RDI. Surprisingly, the velocities doubled over the original field values. The manufacturer was contacted to try to explain the differences between the two methods of referencing. RDI recommended that acoustic bottom tracking be used despite the small compass errors and that the filtering of navigation data be turned off in any further field experiments using differential GPS positions and velocities.

It may be noted from close inspection of the plots for August 26 (Figure 7) that the GPS-based track ended after about two thirds of the experimental period had elapsed but bottom tracking continued until the end of the experiment. An examination of the original navigation file revealed that for some unknown reason the navigation system ceased operating at this point but that the navigation software assumes that the boat is located at the last known position. The irregular track for this experiment indicates where the boat was stopped for temperature profiles.

In order to reduce or eliminate the errors in currents due to compass errors it is recommended to replace the compass by a portable gyrocompass in future underway applications.

4. Analysis of Discharge in the Narrows Region

On four occasions over the experimental period ten second averages of current profiles were recorded while the launch traversed between two Scotsman float markers on opposite shores about a kilometre east of the Arrow Park cable ferry crossing at a speed of around 5kts. The location of this experimental site is shown on Figure 1. Thus, profiles were typically 25m apart. The differential basestation was set up on each of the four days experiments on the southern shoreline at a site indicated to be a CHS bench mark. However, in these experiments the actual bench mark was not located so that the absolute positions were not the same over the four occasions the basestation was operated. During an experiment the relative positions were considered to be accurate to within the specifications of the navigation system. For the combination of the Novatel basestation and Magnevox 300 receiver the accuracy is about 1m (R.Rowsell, pers. com.). On account of the importance of the flow measurements in the narrows for calibrating an indirect method of determining the exchange between the Upper and Lower Arrow Lakes employing water temperature recorders at the Scotsman floats, the profiler velocities, V, normal to the track were summed over the cross section, S, in accordance with equation (1) to yield the total discharge in two different ways, one by the bottom tracking and algorithms supplied by the instrument manufacturer and the other by GPS positions and a simple cross sectional summation of the flow. The discharge across the section, Q, is given by

$$Q = \int_S V.nds \qquad (1)$$

where the unit vector, n, is normal to the transect, taken here as 265°, chosen from visual inspection of the launch trajectory plots (Figure 7).

(a) DGPS method.

Flows components along the 85-265 ° axis with the downstream direction (265 °) taken as positive were summed in 25m wide bins and at each 0.5m depth interval along the transect for each crossing. The number of crossings in the average ranged from 2 to 6 depending on the experiment. All bin entries had to have an error velocities less than 4cm/s, otherwise they were not counted. This meant that bins having depths in excess of 20m sometimes contained no valid data. For these bins either the valid bin average from the bin above was inserted into the missing bin or if the value at the location above was missing too the value of the flow component averaged over the entire depth was inserted into each missing bin in these rare cases. For the 1200KHz device with 0.5m deep bins the standard deviation of an individual reading or ping is reduced by averaging over the 10s sampling interval to 1.55cm/s. Speed may be underestimated in bins located within 15% of the bottom depth and have errors larger than the nominal error of 1cm/s. As well, the average bottom-tracked depth based on the four-beam average depth and horizontal position of each profile was calculated for each 25m-wide bin.

The depth sampling of the current profiler is regular after the first 1.8m depth. In this upper portion no data were measured in allowance for sensor head immersion and near field effects. The discharge was calculated by assuming that the flow in the first bin at 1.8m depth applied over this layer. At deeper depths the average flow in each bin was estimated from the average of flow just above and below the bin. Integrations continued until the bottom depth was reached. The number of 25-m wide bins varied from 35 to 40 with most experiments being 38. Thus, there were typically about 1500 points in each discharge calculation consisting of up to about 100,000 individual velocity measurements.

(b) Manufacturer (RDI) method.
The distance, s, in equation 1 is estimated from the ship velocity as determined from acoustical bottom tracking and the time between profiles of 10s. The manufacture provides software to estimate the flow in the unmeasured upper 1.8m and in the lower depths beyond the range of the instrument. There are two methods, a constant method, whereby the unmeasured flows are extrapolated from the first good bin either upwards or downwards and a power method were the missing data is assumed to obey a user supplied power law. For this study the constant method was chosen in case the flow differed from the usual riverine flow laws. The manufacture also allows for estimation of the discharge in the missing nearshore region from the last valid profile to the bank. With the large number of bins it is considered that the two missing contributions at the shoreline were so small that they could be safely ignored in the calculation in (a). For further details of the manufacturer's method the reader is referred to the Transect Manual provided for using the TRANSECT software, a program that displays ADCP data on a computer screen while underway and also calculates discharge for river applications.

Results
The averaged data for each of the five experiments in the Narrows region is presented in contour form in Figures 8. Experimental times are indicated in UCT. The contour plots were produced by the public domain software package, PGPLOT, using the subroutine PCONX, for plotting contours in irregular regions. An unusual feature of this routine is that it does not require interpolation of the data from the irregular to a regular grid. Instead, the location of the contours is found in the actual space, here the average horizontal location for each bin and the sample depth. This explains why isotachs are not indicated at depths less than 1.8m; the routine does not extrapolate data into missing regions. Negative contours are drawn as dashed lines, for example in Figure 8c. PCONX had to be modified to allow for the labelling of contour intervals in irregular regions.

Patterns of flow from one day to the next are remarkably stable. Flows generally less than 0.2m/s indicated that the Narrows flow is subcritical (Froude Number 0.13). The peak or core of the downstream flow is located at depths from 5 to 10m except on August 26 where it appears to be at the surface. In terms of height above the bed the peak velocity is about 60% of the depth. This position for the peak flow was found theoretically in the mathematical model of open channel flow of Naot and Rodi (1982). Winds were light or moderate for the five experiments so why the core is not always at the surface as would be the case with pure riverine flow warrants further investigation. There is no indication of any flow reversals that might be expected during the coincidence of the highest stratification and the deepest depths in the Narrows. Thus, at other times of the year the exchange is likely to be from the Upper to the Lower Arrow Lake as assumed in the thermal modelling of Hamblin (1997).

Discharges estimated by method (a) are indicated on each figure in the box and by method (b) in parentheses. In four of the five experiments method (b) gives higher discharges than (a). These two estimates provide some estimation of the errors associated with the discharge calculations. Discharges were estimated on a daily basis from the water budget using inflow, outflows, water level changes and basin hydrology by Pieters (pers. com.). It is evident from Table II that the daily water balance method underestimates the discharge as determined from method (a) by 4.5%. This is considered excellent agreement for two independent methods, especially as the water budget method is based on some ungaged inflow to the Upper Arrow Lake and possible diurnal variations in Revelstoke releases are not accounted for. Another source of difference is the wind generated exchange flow which cannot be accounted for in this water balance approach as the water level differences between basins were not determined.

Date , Time (UCT)	ADCP Transport (m^3/s) Method A	ADCP Transport (m^3/s) Method B	Daily Water Balance (m^3/s)
August 21	1921	2187	1832
August 22 17:25-18:33	2124	2034	1876
August 22 19:44-20:52	2089	2373	1876
August 26	1973	2144	1911
August 28	1823	2155	1993
Average	1986	2178	1898

Table II Discharge in the Narrows Region estimated from ADCP current data and from the Arrow Lakes water budget.

Analysis of Averaged Profiles and the Velocity-Dip

The discharge in the Narrows Region was estimated at three day intervals over a 35-day period starting on August 19 by an indirect method using water temperature profiles at each side of the cross section, (Pond, pers. com.). In order to validate the indirect method, profiles of measured flow now in the direction 85^0 and averaged across the channel were plotted in Figure 9. With the exception of the more conventional riverine profile of the August 26 case all profiles had a significant deviation from logarithmic (see Figure 9c) at the surface in accordance with the indirectly measured profiles.

It would be desirable to extract information from the velocity profiles that would permit the estimation of conditions under which the flow in the Narrows would reverse and to estimate the downstream distance in which a substance introduced at the surface would spread vertically over the water column should fertilizer by added at either one of the two ferry crossings in the Narrows region. This is accomplished by fitting a model of the flow profiles based on the likely causative forces.

One of the striking features of the contoured plots and cross sectionally averaged profiles (Figures 8 and 9) is the subsurface peak in the downstream flow at a depth of approximately 8 m and decrease to the surface of about 7cm/s. The winds during the Narrows experiments were generally light and variable and not necessarily in an upstream direction so wind alone cannot explain the observed "velocity-dip". A possible explanation is the difference in water density between the Upper and Lower Lakes. According to an unpublished data report by Pond in all cases the mid lake water temperatures in the upper 10m were up to 5°C warmer in the Lower Lake than the Upper Lake. As well, at the current meter at 6m depth in both lakes, north/south oscillations in the flow of amplitudes about 15cm/s and periodicities of about 3 days. Such oscillations could depress or elevate the stratification in the Narrows region by an estimated 6m. These excursions could change the temperature at these sites by another 2°C. Thus, it is possible that the temperature contrast between the surface waters near the entrance and exit of the Narrows could at times be as large as 11°C. The lighter downstream water would tend to flow over the heavier upstream water resulting in a decrease of flow at the surface. This possibility is included in the model formulation as an internal pressure term.

Mathematical Model

The governing equation for downstream flow profile, u(z) is proposed.

$$\frac{\partial}{\partial z} u_* \kappa (h-z) z / h \frac{\partial u}{\partial z} = Px - \frac{g}{\rho} \int_0^z \frac{\partial \rho}{\partial x} dz \qquad (2)$$

where u_* is the square root of the bed frictional stress, κ, the von Karman constant of 0.4, the free surface pressure gradient is Px, the internal pressure gradient is vertical integral of the horizontal density gradient, $\frac{\partial \rho}{\partial x}$, and g is the acceleration of gravity. The parabolic distribution of vertical eddy viscosity assumed in (2) is standard for rivers. However, the u_* may be effectively reduced by the stratification of the water column. It is assumed that the bulk Richardson number which allows for the reduction of vertical mixing by stratification is independent of depth. Equation 2 has the solution in the case of no surface stress and a constant of integration, z_0, and when the horizontal density gradient varies linearly with the height z above the bottom,

$u(z)=u_*/\kappa \ln(z/z_0)-b_x h/(3u_* k)(hz+z^2)$. The factor b_x equals $g/(2\rho)\frac{\partial \rho_z}{\partial x}$ where ρ_z is the vertical density gradient.

The three unknown parameters in the above solution of equation (2) were determined by a least squared error analysis between the model and the cross sectionally averaged observations. Once the pressure gradients are evaluated then the bed friction may be estimated to yield u*. $u_* = \sqrt{hpx - h^3\frac{bx}{3}}$. The best fit parameters are listed in Table III for the five experiments. The best-fit current profiles are compared to the averaged profiles of current observations in Figure 10.

Date, Time	$px X10^4 (m/t^2)$,	$bx10^6 (m^{-1} t^{-2})$,	z_0 (m)	u_*(m/s)
August 21, 21:38-22:15	0.580	1.53	0.8	.0274
August 22, 17:25-18:33	1.21	4.39	0.85	0353
August 22, 19:44-20	0.32	0.197	0.72	.0243
August 26, 19:53-21:54	0.40	0.0	1.1	.0283
August 28, 00:38-00:56	0.33	$0.65X10^{-5}$	0.96	.0257

Table III. Best-fit parameters to average velocity profiles.

Discussion and Application

The internal pressure gradients are largest for the first two cases when both the observations and model have a clear surface velocity maximum. The horizontal reduced density gradient would be 2x10-9 ($m^{-1} t^{-2}$)in this case assuming a Narrows length of 40 km. Such a density gradient appears to be too small compared to bx by two orders of magnitude. Owing to the great length of the Narrows it appears that internal pressure gradients, that might arise from density differences between the two lakes, are far too weak to cause the near surface decrease of flow.

The surface pressure gradient is equivalent to downstream slope of over 1cm in a kilometre on August 22 but in the other cases the slopes are considerably less. If this slope persists throughout the Narrows there could be a difference in water level in the two lakes of up to 40cm.

The values of z_0 appear to be much too large which indicates that the velocity profiles deviate considerably from the logarithmic boundary layer flow. On August 26 when there was no near surface decrease and the flow was driven by surface pressure only the largest

z_0 occurred. It is possible that the flows within 3m of the bottom are underestimated due to side lobe contamination of the doppler shifts. As a test the near bottom flows were doubled with the effect that z_0 was decreased somewhat.

As the mixing in this shallow water column is generated by shear at the bed it is likely the that inferred values of u_* are reliable. They are consistent from one experiment to another with a characteristic value of 0.03m/s. This value of u_* is surprisingly high in consideration of the density stratification to be examined shortly.

Once the distributions of velocity and vertical eddy viscosity are known, the evolution of a substance added at the surface can determined from the advective diffusion equation. Since there are no analytical solutions and a numerical model is beyond the scope of this report a scaling analysis is performed. It is well known that the vertically averaged eddy coefficient in a river is 0.06 u_* h. The characteristic time taken for a substance introduced at the surface to mix to the bottom is $h/(0.06\ u_*)$. At a typical average downstream speed of 0.1m/s the introduced substance would reach the bottom in about 1 to 2 km from its point of origin. Thus, it may not be desirable to add nutrients in the the Arrow Park ferry crossing Narrows Region as they would be rapidly mixed over the water column permitting uptake by the benthic community before they reached the Lower Lake.

The question of the velocity-dip or decrease in flow near the surface remains. To account for the observed near surface current shear of $10^{-3}\ s^{-1}$ a wind speed in excess of 10m/s directed upstream would be required based on the above value of the eddy viscosity and the usual wind drag coefficient. As this wind is far too high an alternate cause is examined below. But first, an analysis of the temperature data collected on August 26 follows.

Due to difficulties with the OS-200 profiler temperature profiles coincident with velocity profiles were measured only on August 26. Unfortunately, this was the only day when the velocity-dip was not detected. However, it is assumed that the general conclusions found on this day apply to the other days as well. Six locations evenly spaced across the Narrows study area were programmed into the DGPS navigation software, permitting accurate repeated station keeping on each transect of the survey vessel. Altogether, each station was visited five times but due to an unknown fault in the DGPS electronic navigation system, only the first three station occupations had accurate locations and were used in the subsequent analysis. Although the bottom tracked velocities could have been integrated to give position, Figure 7 demonstrates that this would lead to unacceptably large errors in position.

Averages of temperature and ADCP profiles, positions and depths were computed at each of the six locations. These data are displayed in profile form in Figure 11 and as contoured isopleths in Figure 12. The stability frequency is a measure of the rate of density stratification and is based on the vertical gradient of density divided by density and multiplied by the acceleration of gravity. Water density is computed from temperature according to the expression of Chen and Millero (1977) for lake water. The

Richardson number is defined as the stability frequency divided by the sum of the squares of the vertical shear of the two horizontal velocity components and is a measure the degree of turbulent mixing in the water column with values of 0.25 or less being associated with active turbulent mixing. Figures 11 and12 indicate that over most of the water column except near the boundaries the shear is insufficient to generate turbulence.

Based on the data of Figures 11 and 12 the geophysical setting of the Narrows channel can be established. The balance of Coriolis and buoyancy forces may be compared roughly through the ratio of the stability frequency to the Coriolis parameter, which is 1.05 10^{-4} s^{-1} at a latitude of 50° N. Thus the Coriolis forces are two orders of magnitude weaker than the buoyancy forces. Alternatively, these forces may be compared by the ratio of the internal Rosby radius of deformation to the channel breadth. The Rosby radius is the phase speed of the internal wave divided by the Coriolis parameter. The appropriate phase speed for the Narrows is the product of the stability frequency and the mean depth yielding a value of 0.4m/s. The channel breadth of 800m is about one fifth of the Rosby radius meaning that, again, rotational forces are weak in comparison to buoyancy forces. Nonetheless, Figure 12 shows a deflection of the more cold and dense water to the southern shoreline which demonstrates the influence of Coriolis forces. This was also found in the isotherm plot of Hamblin and McAdam (1997) in the Narrows. Despite the weakness of Coriolis forces, the dynamic method has been used successfully by Hamblin (1997) and by Pond (per. com.) to infer along channel isotach distributions and transport through the Narrows.

Having established that the Narrows flows are strongly stratified the discussion of the velocity-dip continues. Velocity dips are common in open channels with ratios of breadth to depth up to 5 (Nezu and Nakagawa, 1993). They and others have shown by mathematical modelling that the dips are due to forcing of a secondary circulation in the vertical plane spanning the channel by turbulent Reynolds stresses which cause low downstream velocity fluid to be ejected from the nearshore regions across the upper surface to the interior. A strong downflow that occurs at the channel centre causes the velocity-dip as momentum is transported from the free surface toward mid-depth. They found that in wider channels such as the Narrows with an aspect ratio of 40 that a number of cells are generated with a horizontal spacing of twice the depth. However, to the knowledge of the author the geophysical case of strong stratification and weak turbulence and rotation has not been studied. In estuaries it is likely that secondary circulation is dominated by tidal effects. It is possible that the stratification reduces vertical motions and causes the two near surface flows of low downstream velocity to meet at mid channel regardless of the breadth.

Observed horizontal components of secondary flow are examined for all Narrow experiments in Figure 13 in order gain some understanding of the velocity-dips. Unfortunately, due to the directional uncertainty of the ADCP discussed in section 3 errors in the cross stream component of flow are at least 1cm/s, a much larger relative error than in the downstream flow where errors are in the range of 5 to 10%. In any case, layers of northward flow (positive sign) alternating with southwards flow (negative sign) tend to extend across the channel rather than meeting at mid channel. This could be a consequence of density stratification constraining the cellular motion found in unstratified open channel flow. No apparent tendency for the nearsurface advection of low velocity fluid from the shallow nearshore region is seen so the observed secondary circulation does not support the near surface velocity-dips. Vertical flows are also measured by the ADCP and one example was plotted (not shown).Vertical components of flow are below the detection limit of the ADCP profiler.

5. Inflow Region

The inflow region is considered of interest to the question of the introduction of fertilizer. Nutrients should not be added to the mainstem Columbia River upstream of the Upper Lake if the river inflow plunges below the photic zone.

Figure 14 shows the locations of the four transects logged over the three and a half hour long experimental period. The first three were located in sufficiently shallow depths to permit bottom tracking. This explains why the launch trajectory in the third transect is curved. The first transect was intended to measure the flow in the main inflow channel into the Upper Lake. The submerged inflow channel divides into two banches. Unfortunately, time constraints allowed for only one branch to be surveyed. The purpose of the second transect was to examine the possibility of exchange between the main lake and Beaton Arm and for the third, the observation of the inflow into the main lake was the goal. In the first three cases individual profiles were first averaged over 100m-wide bins along the ship trajectory before contouring. Another transect was observed for the purpose of tracing the inflow in the open lake. Unfortunately, at transect four the depth was too great for bottom tracking so that no ADCP measurements were taken.

The flow along the inflow channel is evident in Figure 15 to be concentrated along the bottom and at a temperature of 10 to 12^{o} C, considerably colder than the surface temperature. At the point along the transect where it joins another channel at about 1200m from the start, the flow reduces rapidly, indicating that a sizeable portion of the main inflow likely takes the unsurveyed branch. Another interesting feature is a near surface inflow of warmer water which may be the source of similar surface jets seen on the other two transects. Similarly, it is most pronounced at the junction of the two branches suggesting that it too flows mainly into the other branch of the submerged inflow channel. Finally, there is a pronounced tilting of the thermal structure along the transect with colder and heavier water in a downstream direction. This sloping structure was not observed by (Hamblin and McAdam, 1997) so that it may be a transient situation due to wind forcing in Beaton Arm.

Exchange with Beaton Arm is apparent in Figure 16 with warm water flowing in and colder water flowing out of the Arm. Altogether, there is a net inflow at the time of measurement of approximately 600 m^3/s. From the depth soundings of the ADCP the inflow channel surveyed in Figure 15 is found from 100 to 700m while a broad bank separates it from the other at a position of 2200m. The exchange flow is located near the mouth of this second inflow channel reinforcing the conclusions drawn from transect one. Somewhat cooler temperatures occur along the southern shoreline.

The main Columbia River inflow is clearly shown in Figure 17 as a plunging jet with a core located at a depth 13m and along the western shoreline. This tendency for inflows to hug the right hand side of the channel in the northern hemisphere has been noted in other long narrow lakes (Hamblin and Carmack, 1978) and is thought to be due to the earth's rotation. This jet must have paralleled the 10m isobath in general as it crossed the inflow area from the mouth of the western branch of submerged channel in a southwesterly direction. A much weaker two-layer jet is found near the surface over the clearly distinguished submerged inflow channel. This feature is similar to the surface inflow and subsurface outflow of Beaton Arm which suggested that it originates in the second inflow channel but bificurates at the end of the channel into two branches. The total discharge across the channel was 1062 m^3/s at the time of the experiment. Most of the discharge is concentrated along the western shoreline. In the upper panel of Figure 17 the rate of stratification is accentuated on the western shoreline with warmer water at the surface and colder water at depth. The core temperature of the inflow jet along the western shoreline is approximately 10.3°C.

At transect four eight profiles of temperature were used to produce the contoured temperature and inferred flow distributions shown in Figure 18 At this location two kilometres downstream from transect three the pronounced cross channel temperature gradient seen at transect three is not evident. Nevertheless, an attempt was made to deduce the flow across the transect from the dynamical method described by Hamblin (1997) and applied to temperatures measured in the Narrows region. The discharge across the section needed to establish a reference velocity was assumed to be the value measured at transect three. In order to evaluate the accuracy of this method in a less confined area than the Narrows region, the same method was applied to transect three where the flow was directly measured. On account of the poor correspondence between the indirectly determined flow of Figure 19 with the measured flow of Figure 17, it is concluded that the distribution of flow shown in Figure 18 is not reliable. Both plots fail to show the expected Columbia River inflow jet. Based on temperature alone it would appear from Figure 18 that the depth of the core of the inflow is about 20m. Thus, the inflow would likely be below the photic zone. In future work, a more sophisticated theoretical approach should be developed to estimate the flow across transect four. In hindsight, relative ADCP measurements across transect four should have been observed which could have yielded at least qualitative information on the nature of the inflow as it reaches the open lake.

6. Comparison of ADCPs and Electromagnetic current meter.

Comparisons of the 1200 and 300 KHz ADCPs were conducted in the Lower Arrow Lake (Hamblin, 1998) but due to logistical difficulties the results were somewhat inconclusive as the two instruments were not operated concurrently. However, the 1200 KHz model compared favourably with a moored electromatic current meter but the 300KHz did not. At the mid lake temperature and current meter mooring on August 25 (Figure 1) another comparisons was made while tethered to the surface meteorological float. The purpose of this comparison was to evaluate further a 300 KHz ADCP for suitability for use in the Arrow Lakes Reservoir and to compare both instruments to the two electromagnetic current meters moored at the location at depths of 6 and 50m. Potentially, the 300 KHz ADCP has greater range than the higher frequency model. The electromagnetic current meter, model S4, was operated by the University of British Columbia and manufactured by InterOcean Systems Inc. From speed and direction data of the S4 current meter at 6m kindly supplied by Dr. S. Pond (pers. com.) and presented in Table IV it is apparent that the flows were steady at a mean speed of 2.5 cm/s and direction of 220° during the period of comparison.

At the centre of the Upper Arrow Lake the water is far too deep for bottom speed reference of the 1200 KHz model and the 300 KHz instrument lacked bottom tracking. However, a base-station differential GPS provided estimates of the drift velocity of the surface buoy and attached survey vessel. Figure 20 depicts the trajectory of the survey vessel during the 1200 KHz experiment. The locations of the 10-min averages are indicated. Based on 10-min averages the maximum drift speed was 1.0cm/s while the average was around 0.5 cm/s. Averaged drift velocities were subtracted from the 10-min averages of the 1200 Khz ADCP and the 300KHz during the concurrent period, 19:41 to 20:50.

On August 25, the 300 KHz device registered meaningful velocities as deeply as 90m but not at the 0.5m depth resolution of the higher frequency profiler but rather at 3m depth intervals. This is in contrast to the August 20 case (Hamblin, 1998) when the depth interval was 1m. The maximum possible range of the lower frequency meter 384 when set to resolve 3m bins. While usable velocities were not detected at depths below 90m, acoustic backscatter intensity peaked at the 300m bottom depth suggesting the sound reflected off the bottom was observed. Thus, acoustic bottom tracking with this model of the ADCP may be possible throughout the lake. Comparisons of 10-min averages of velocity profiles of the two models are provided in Figure 21. For the overlapping period from 19:46 to 20:06 there is close correspondence over the upper 3 to 15m of the water column where most of the flow is concentrated. Agreement of the two ADCP profilers with the electromagnetic current meter is reasonable considering that the electromagnetic current meter recorded 1-min averages of flow every 20 minutes.

300 KHz ADCP	Time(GMT)	East (cm/s)	North (cm/s)	S4	Time (GMT)	East (cm/s)	North (cm/s)
	19:41-19:51	-3.8	9.5		19:40	1.5	10.6
	19.51-20:10	-5..3	8.9		20:00	-0.1	8.9
	20:10-20:30	-5.8	8.6		20:20	-8.1	7.1
	20:30-	-4.5	7.2		20:40	0.0	9.7

	20:50						
	20:50-21:00	-3.1	5.7		21:00	-5.3	10.0
1200 KHz ADCP	19:41-19:51	-6.4	10.7		19:40	1.5	10.6
	19.51-20:10	-7.5	11.4		20:00	-0.1	8.9
	20:10-20:30	-11.0	12.5		20:20	-8.1	7.1
	20:30-20:50	-9.5	10.9		20:40	0.0	9.7

Table IV. Comparison of ADCP and S4 currents at 6m depth mid lake on August 25. The two ADCPs are continuous averages over the period indicated while S4 are 1-min averages every 20 minutes.

At the 50 m depth both the 300KHz ADCP and the current meter show in Table V weak flows not exceeding 3cm/s. Although the agreement in speed is reasonably it is likely that the relative noise at such low speeds results in poor directional correspondence.

300 KHz ADCP	Time(GMT)	East (cm/s)	North (cm/s)	S4	Time (GMT)	East (cm/s)	North (cm/s)
	19:41-19:51	-0.9	0.2		19:40	0.9	-3.3
	19.51-20:10	-0.1	3.1		20:00	2.4	1.1
	20:10-20:30	-1.6	0.0		20:20	-0.5	0.5
	20:30-20:50	-1.6	-0.7		20:40	1.6	0.1
	20:50-21:00	-0.8	-1.2		21:00	-1.3	0.2

Table V. Comparison of ADCP and S4 currents at 50m depth mid lake on August 25. The ADCP is a continuous averages over the period indicated while S4 are 1-min averages every 20 minutes.

7. Effects of Compressiblity on Temperature Profiles

Hamblin and McAdam (1996) noted in their survey of water temperatures in the Upper Arrow Lake Reservoir that near-bottom temperatures in the deeper areas were lower than the temperature of maximum density of pure water of $3.98C^{o}$ .The temperature profile taken on August 27 supports the earlier observations at the deepest location in the lake. Unfortunately, the OS200 profiler was not capable measuring the lower 60m of the water column due to the limitations of its design range. A comparison is given in Figure 22. along with the decrease in the temperature of maximum density with depth according to Farmer and Carmack (1981) for reference. It is apparent that the temperature distribution in the lower depths is close to thermodynamic equilibrium. This observation supports the inclusion of compressibilty effects on water column stability in the water quality modelling of Hamblin (1997).

8. Conclusions

A high frequency acoustic doppler current meter worked better than anticipated for such a undernourished water body due in part to the relatively high flow. Fortuitously, the study period coincided with a peak in suspended material due either a high input of glacial flour or to increased primary production. The ADCP technology may not perform as well at other times. Although the profiling range was somewhat restricted the bottom tracking range appeared to be enhanced. In order to reduce or eliminate the errors in currents due to compass errors it is recommended to replace the compass by a portable gyrocompass in future underway applications. Even though bottom tracking was not possible in some of areas of interest ADCP data should have been taken in any case rather than relying on the dynamic method which did not work except in the Narrows where the flow is more concentrated.

A lower frequency ADCP yielded reasonable results in the Upper Arrow Lake but at the cost of much reduced vertical resolution. This device has the potential for acoustical bottom tracking throughout the Arrow Lakes Reservoir as there was an indication of bottom reflected signals at the deepest point. Therefore, absolute flows in the upper 90m of the water column could be determined throughout the Arrow Lakes Reservoir. ADCP results from both frequencies compared favourably with two electromagnetic current meters despite the low conductivity of lake water. Unfortunately, water temperature can not yet be measured remotely and underway which results in a severe undersampling of water temperature using traditional techniques. An improved system of temperature profiling capable of more rapid sampling is recommended if currents are to be properly interpreted. The NWRI's OS200 temperature logger should be replaced by a more reliable model.

An application of new electronic positioning technology to the Arrow Lakes appears to be successful despite the mountainous terrain. The differential system greatly reduced the uncertainty in horizontal position and was found to be superior to acoustical bottom tracking for position. In future applications navigational data quality and possibly pseudoranges should be recorded in the navigation data file and all positions should be referenced to the same datum as the chart datum.

Information on the hypsography of the Upper Arrow Lake indicated that former estimates based on similarity to Kootenay Lake were incorrect and that inferences made of the sensitivity to proposed changes in the outflow of the lake may be affected. It is recommended that the thermal modelling be repeated with the new lake geometry and meteorological data measured as a component of this study.

Observations of the flow in the Narrows region suggest it is highly unlikely that there is exchange from the Lower to the Upper Arrow Lakes. Flow in the Narrows is unusual being near-steady, stratified and weakly rotating. Several methods of integrating the flow over the cross section appear to be consistent. A novel observation of a decrease of flow near the surface observed on four of five occasions is likely due secondary circulations driven by the riverine turbulence rather than by wind or internal density gradients.

Despite the limited range of the underway ADCP the circulation in the inflow region was found to have a complex three-dimensional distribution dictated by bathymetric steering, density stratification and the earth's rotation among other factors. A focussing of the flow on the right hand side of the lake in the direction of flow was observed close to the inflow. Whether this effect was due to the earth's rotation or a combination of outflow geometry and bathymetric steering will have to await additional three-dimensional circulation modelling.

The ADCP survey has implications for the optimization of a strategy for the introduction of nutrients. As the mainstem Columbia River inflow enters as an interflow as suggested by Hamblin and McAdam (1997) nutrients would be directed away from the photic zone were they to be introduced in the Columbia River. If the near surface inflow continues downstream for at least 5km beyond transect three then nutrients should be dispersed from the Shelter Bay car ferry at a point half way across the lake. Since a major finding is that transport from the Lower to the Upper Arrow Lake is unlikely, nutrients required for the whole system could be added at the Shelter Bay ferry. However, due to mixing in the Narrows the inflow to the Lower Arrow Lake is likely also to be an interflow. It is recommended that the Lower Lake's nutrient requirements be added from the Needles cable ferry. Hopefully, this location is sufficiently close to the main body of the Lower Lake that nutrients would not be transported out of the photic zone by vertical mixing before they reach the open lake. Additional ADCP measurements and mixing calculations would be useful to confirm this likelihood.

Acknowlegements
The writer would like to thank all those who helped in the field observation and analysis of the data. R. Rowsell of NWRI Research Services Division is thanked for participating in the field. A. Koudys and M. Fououtan of the Canadian Hydrographic Service are thanked for reducing much of the electronic chart data. R. Pieters of the University of British Columbia and G. Thorp of the BC Ministry of Environment, Lands and Parks (MELP) aided in the logistical support for the field study. The author is grateful to Dr. R. Dewey of the Centre for Earth and Ocean Research, University of Victoria, who lent the 300KHz ADCP. Drs. S.Pond and R. Pieters of the University of British Columbia kindly provided helpful comments in the preparation of this report. This study was funded, in part, by MELP through the Columbia Basin Fish and Wildlife Compensation Programme.

References

Ashley, K.I, L.C. Thompson, D.C.Lasenby, L.McEarchern, K.E.Smokorowski and D. Sebastian. 1997 Restoration of an interior lake ecosystem: the Kootenay Lake Fertilization Experiment. Water Qual Res. J. Canada,32(2):295-323.

Chen, C.T and Millero, F.J. (1977). The use and misuse of pure water PVT properties for lake water. Nature, 266, 707–708.

Farmer, D.M. and E.Carmack, 1981. Wind mixing and restratification in a lake near the temperature of maximum density. J. Phys Ocgr. 11:1516-1533.

Hamblin, P.F. 1998 Baseline Physical Limnology of the Lower Arrow Lakes Reservoir National Water Research Institute Contribution 98-238.

Hamblin, P.F. 1997. Preliminary Study on the Impact on the Thermal Regime of Proposed Hydro-Electric Power Development at Hugh Keenleyside Dam on the Arrow Lakes, B.C Unpublished Report NWRI 97-111.

Hamblin, P.F. and S.McAdam. 1997. Temperature, conductivity and wind observations in the Arrow Lakes, B.C.: A Data Report. Unpublished Report NWRI 97-109.

Hamblin, P.F, C.L. Stevens and G.A. Lawrence 1995. Field Experiments with Dye Tracing and an Acoustic Doppler Current Profiler. Proc. Canada/United States Technical workshop on the Upper Columbia River Basin: An International Dialogue State of Wash. Water Research Center, Pulman Wash. 123-128.

Hamblin, P.F. and E.C. Carmack. 1978. River induced currents in a fjord lake. J. Geophys. Res. 83, 885-899.

Naot, D. and W. Rodi. 1982. Calculation of secondary currents in in channel flows. J. Hydraulics Div. ASCE, 108: 948-968.

Nezu, I. and H. Nakagawa,. 1993.Turbulence in open channel flows. IAHR Monograph A.A.Balema, Rotterdam, Brookfield.

Rae,R.M. F.R.Pick, P.B.Hamilton and K.I.Ashley, 1996. Effects of fertilization on phytoplankton in Kootenay Lake, British Columbia. Lake Reservoir Mgmt. 12(2):78-90.

List of Figure Captions

(1) Shoreline of Upper Arrow Lake and study areas.
(2) Outline of the 10m depth contour.
(3) Same as Figure 2 but 50m depth contour.
(4) Same as Figure 2 but 100m depth contour.
(5) Same as Figure 2 but 200m depth contour
(6) Hypsographic curves, mean breadth, area and volume with depth, for the Upper Arrow Lake Reservoir. Solid curve is area, short-dashed curve is volume. X is the area based on CHS chart 3057.
(7) Survey vessel positions on four surveys in Narrows region.
(8) Cross sectional contours of downstream component of flow for experiments of Figure 7. (a) August 21, (b) August 22, 17:25 to 18:33, © August 22, 19:42 to 20:53, (d) August 26, (e) August 28.
(9) Average vertical profiles of flow of the data of Figure 8. (a) against depth, (b) with height above bed, (c) same as Figure 9b except for logarithmic depth scale.
(10) Comparison of averaged observed velocity profiles (solid line) with best-fit model for Narrows experiments (dashed lines).
(11) Profiles at Narrows transect, August 26, 1997. Upper, temperature; middle, stabilty frequency; lower, Richardson number.
(12) Same as Figure 11 but displayed in contoured form.
(13) Isotachs of cross channel flow at Narrows transect for the same experiment as in Figure 8. (a) August 21 (b) August 22, 17:25 to 18:33, © August 22, 19:42 to 20:53, (d) August 26, (e) August 28.
(14) Survey vessel trajectories, August 27. Survey times in GMT.
(15) Acoustic doppler current profiler and temperature data on transect one. Upper panel, isotherms; lower panel, isotachs of downstream component of flow.
(16) Same as Figure 15 but for transect 2
(17) Same as Figure 16 but for transect 3
(18) Same as Figure 16 but for transect 4
(19) Inferred flow across transect 3 from temperature data.
(20) Plot of survey vessel position at mid lake mooring, August 25.
(21) Staggered profiles of east component currents (solid line) and north currents (dashed curve) in cm/s. North components are indicated at the depth marked by an x for the purpose of scale. The relative velocity scale is also given on the x-axis. The central time for each 10-min average is given at the top of the profiles (hr:min).
(22) Comparison of temperature profiles at the mooring (a) this study, (b) after Hamblin and McAdam, (1997). The dashed line is the temperature of maximum density after Farmer and Carmack (1981).

Upper Arrow Lake Shoreline

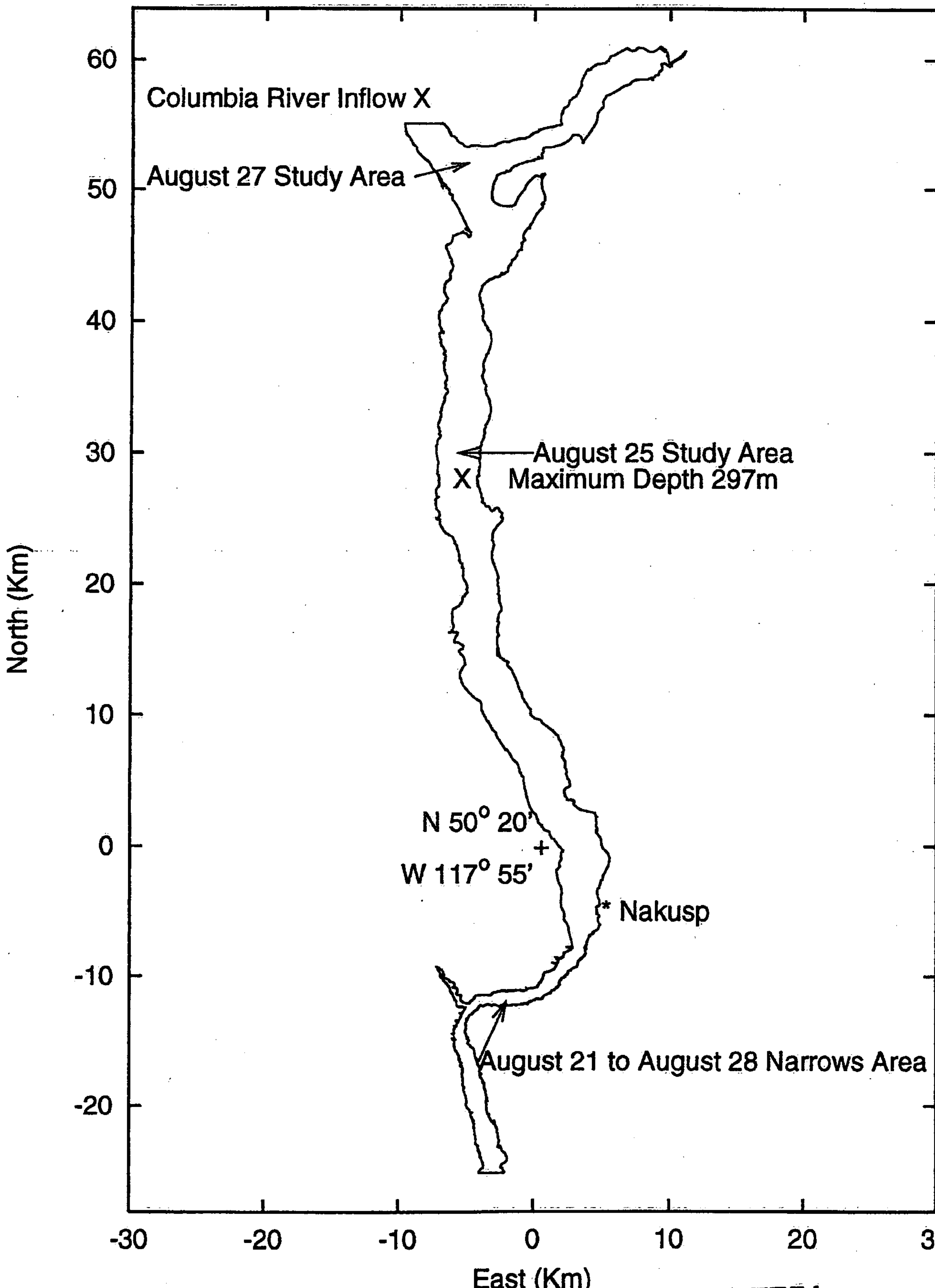

FIGURE 1

Upper Arrow Lake 10m Depth Contour

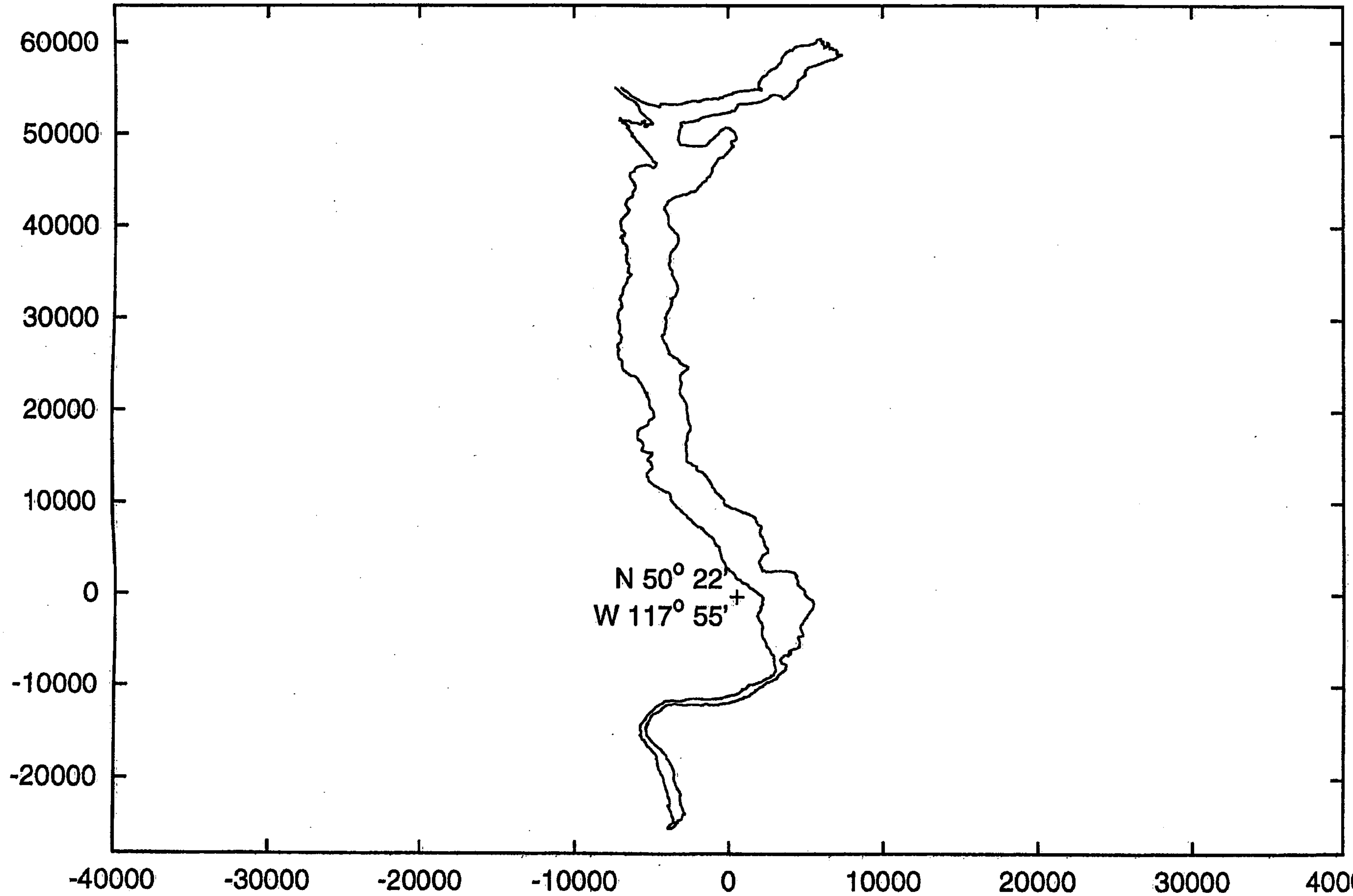

FIGURE 2

Upper Arrow Lake 50m Depth Contour

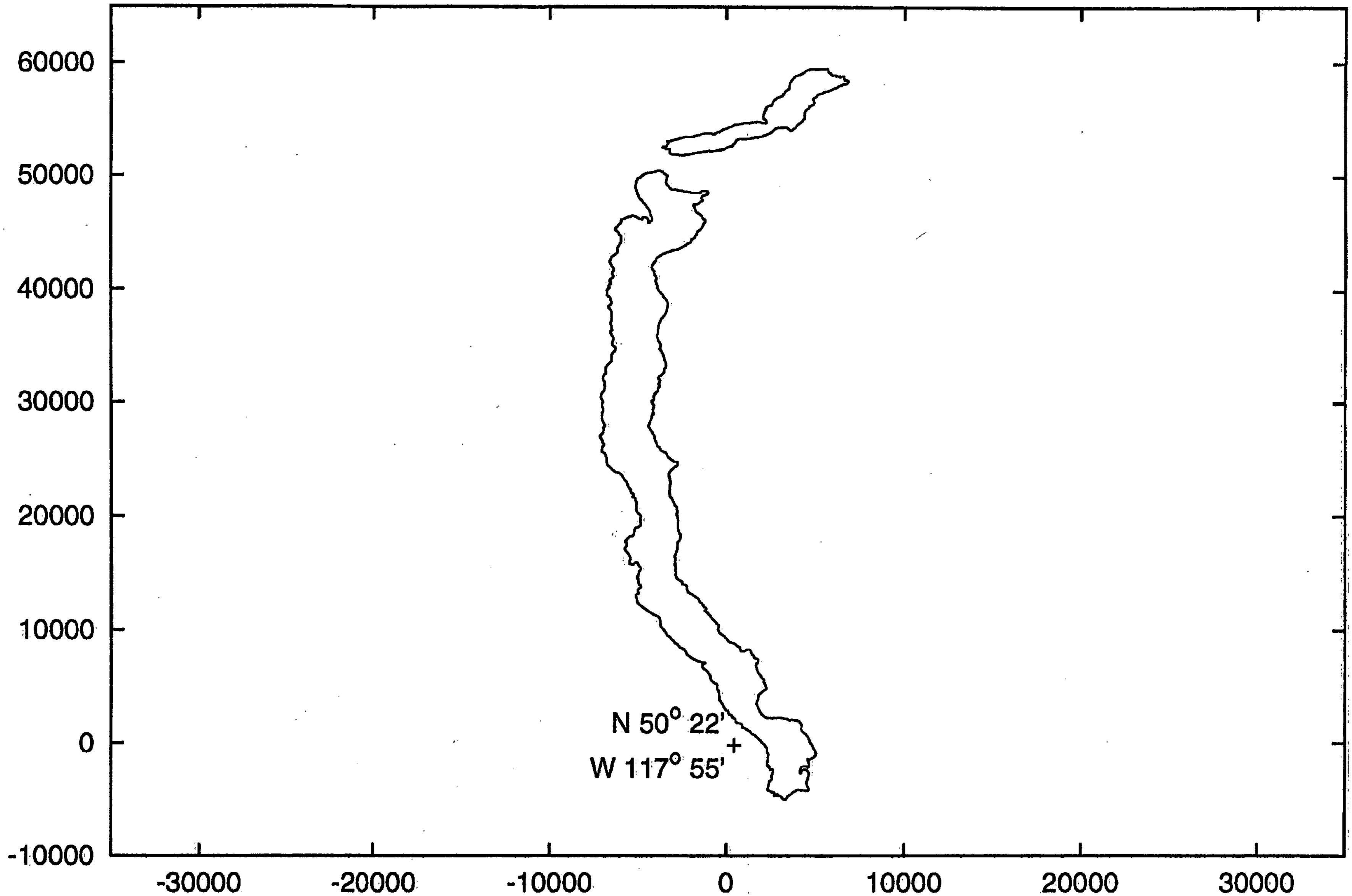

FIGURE 3

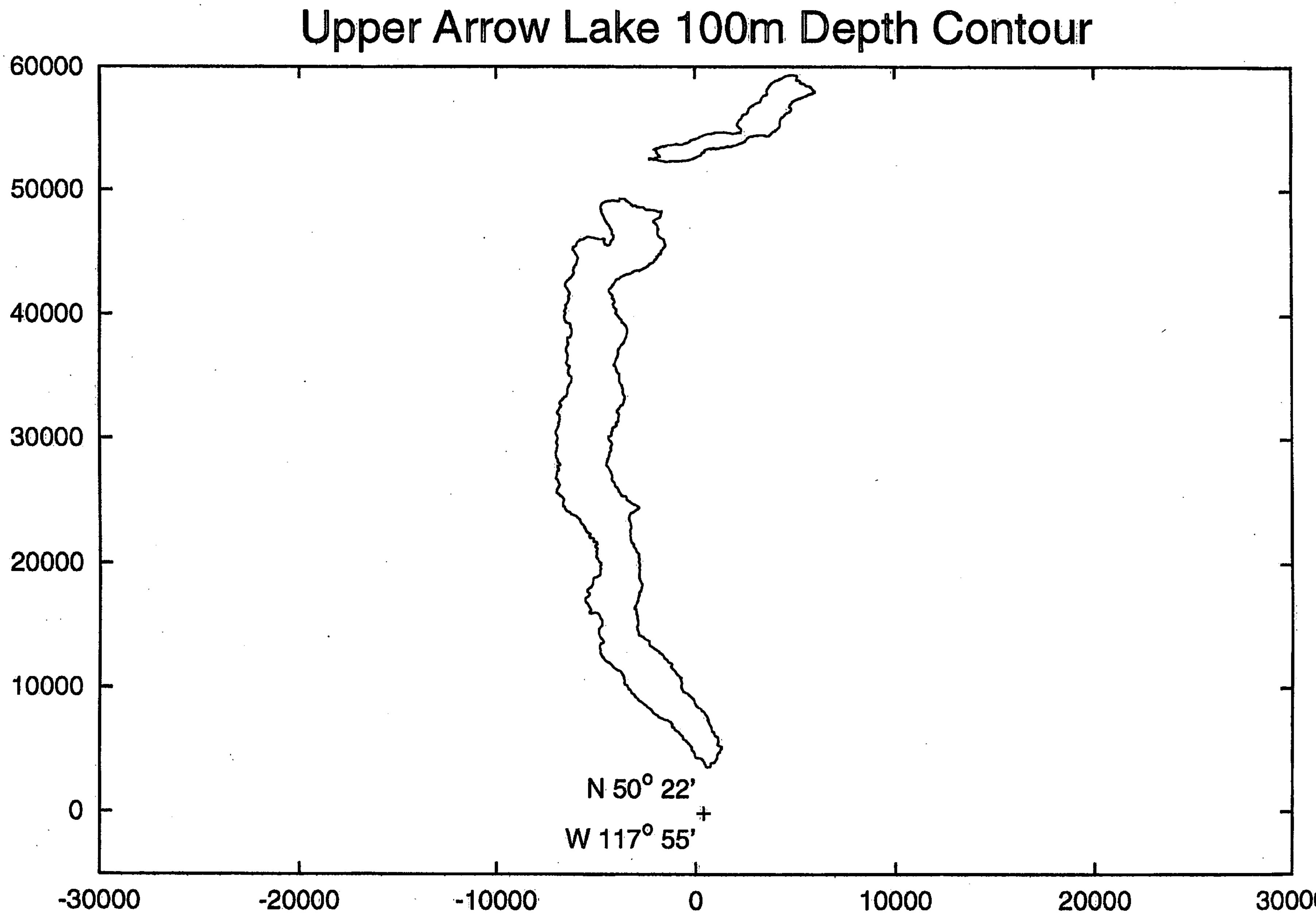

Upper Arrow Lake 100m Depth Contour
60000
50000
40000
30000
20000
10000
0
-30000
-20000
-10000
0
10000
20000
30000
N 50° 22'
W 117° 55'

FIGURE 4

Upper Arrow Lake 200m Depth Contour

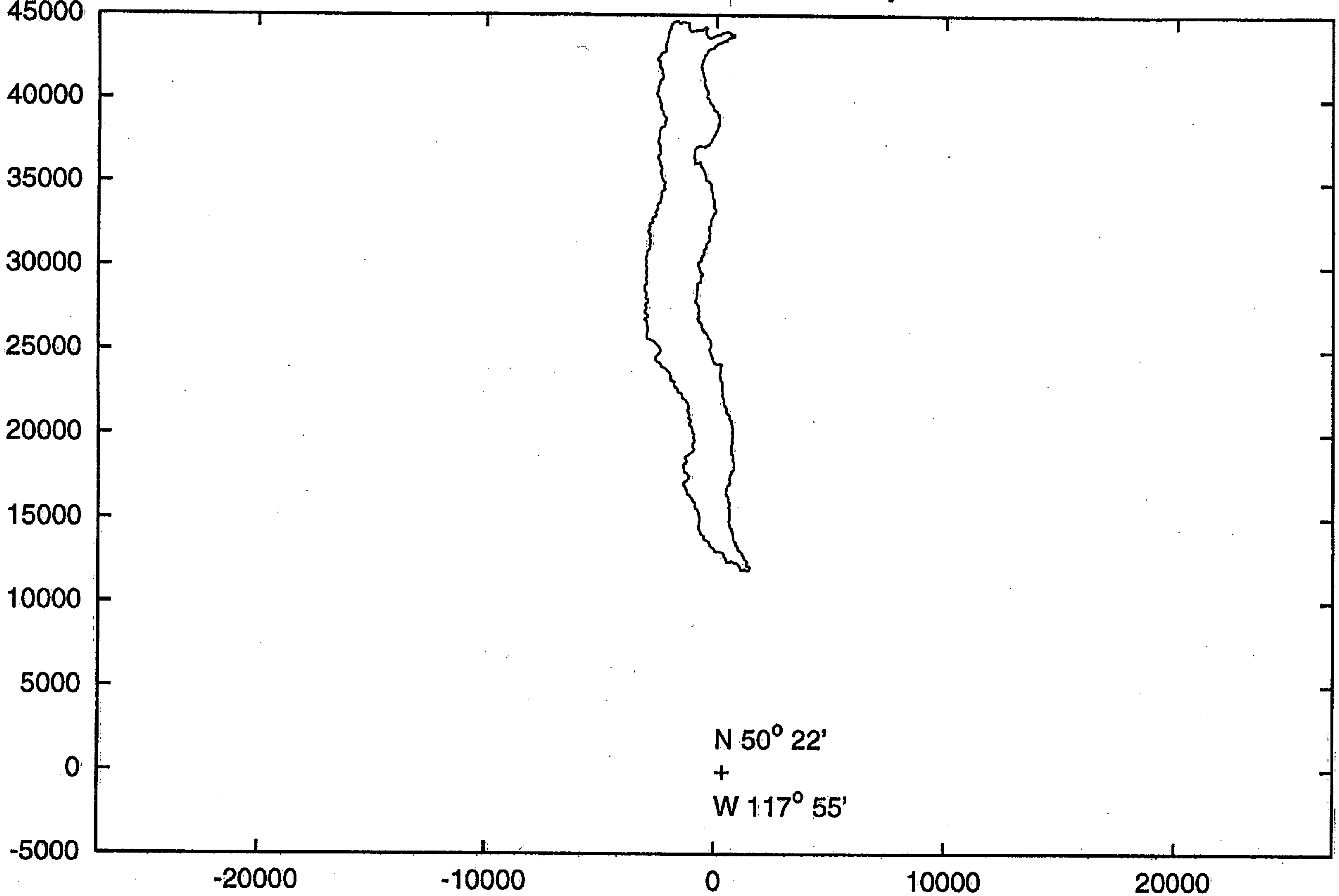

FIGURE 5

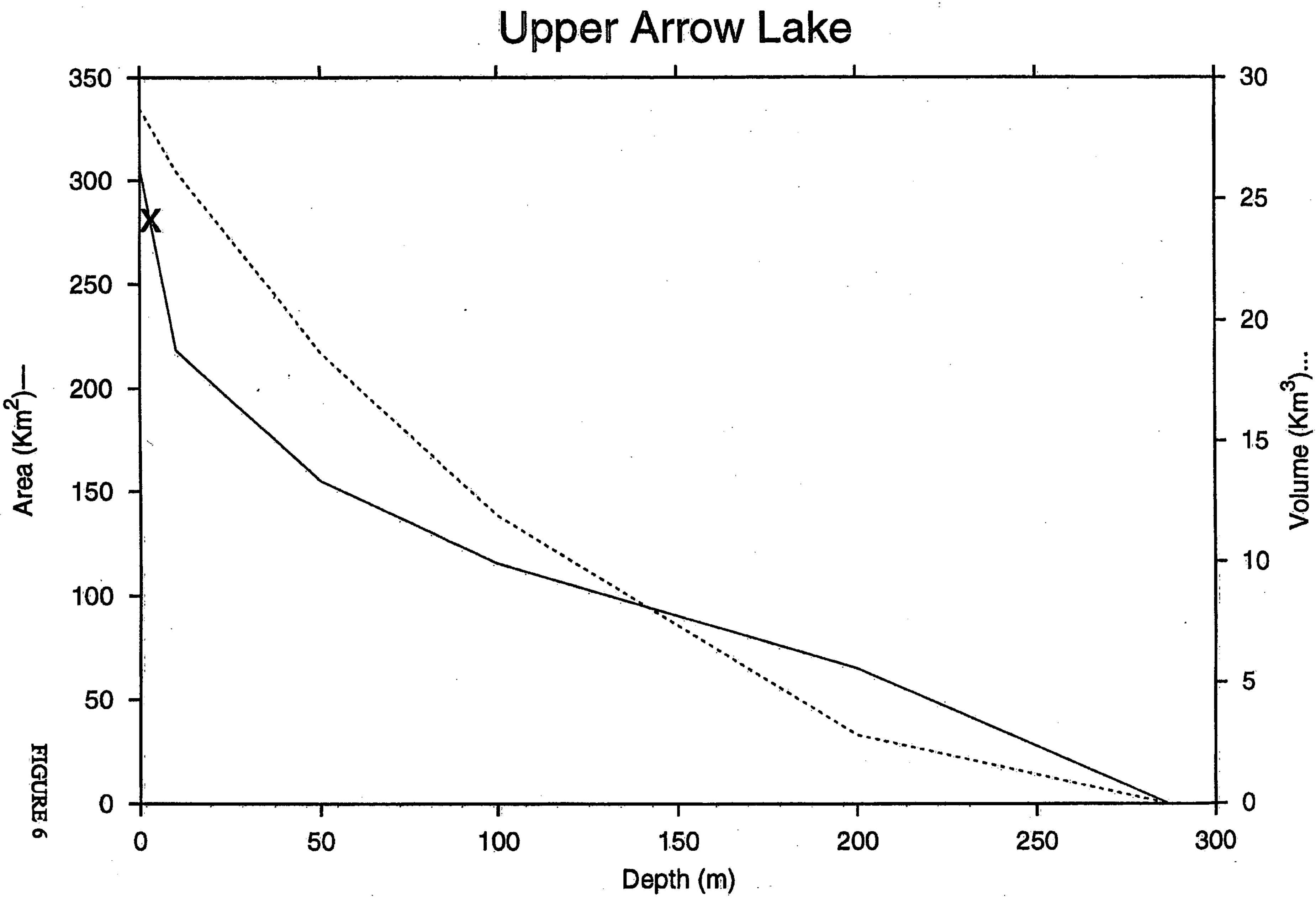
Upper Arrow Lake
Area (Km²)—
Volume (Km³)...
Depth (m)
350
300
250
200
150
100
50
0
30
25
20
15
10
5
0
0
50
100
150
200
250
300
X

FIGURE 6

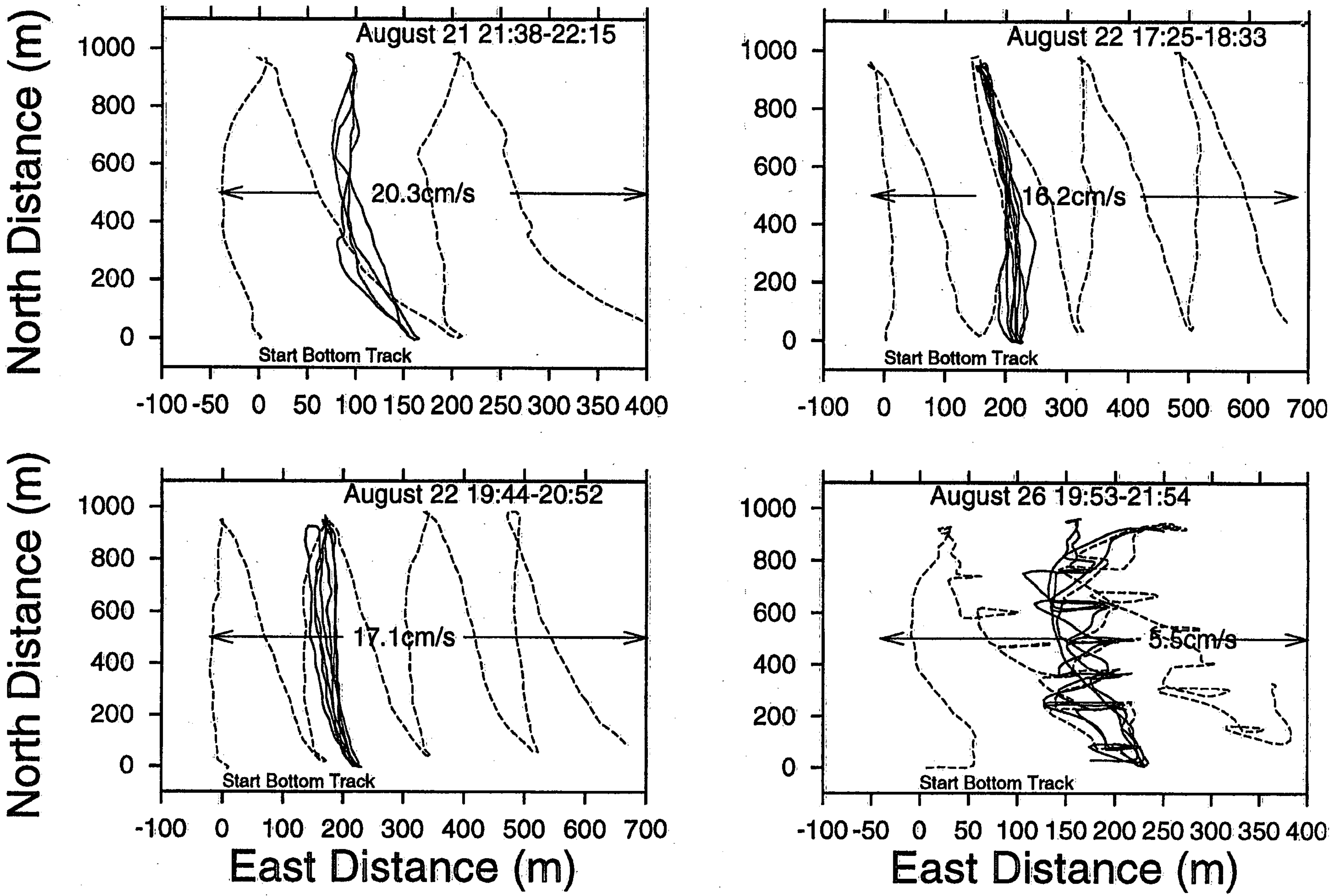
August 21 21:38-22:15
20.3cm/s
Start Bottom Track
August 22 17:25-18:33
16.2cm/s
Start Bottom Track
August 22 19:44-20:52
17.1cm/s
Start Bottom Track
August 26 19:53-21:54
5.5cm/s
Start Bottom Track
North Distance (m)
East Distance (m)
-100 -50 0 50 100 150 200 250 300 350 400
-100 0 100 200 300 400 500 600 700
0 200 400 600 800 1000

FIGURE 7

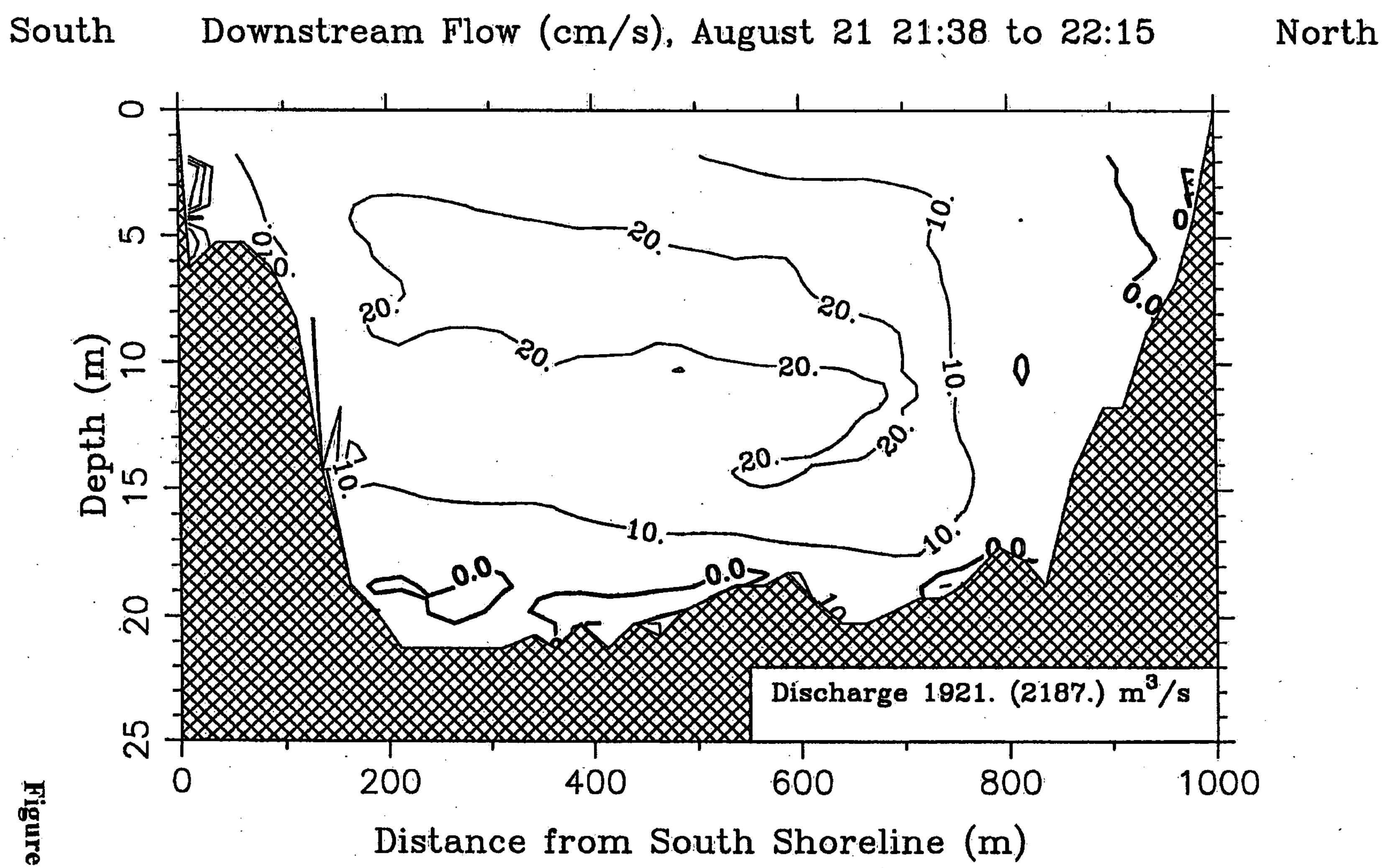
South
Downstream Flow (cm/s), August 21 21:38 to 22:15
North
Depth (m)
0
5
10
15
20
25
0
200
400
600
800
1000
Distance from South Shoreline (m)
20.
10.
0.0
Discharge 1921. (2187.) m3/s

Figure 8a

South Downstream Flow (cm/s), August 22 17:25 to 18:33 North

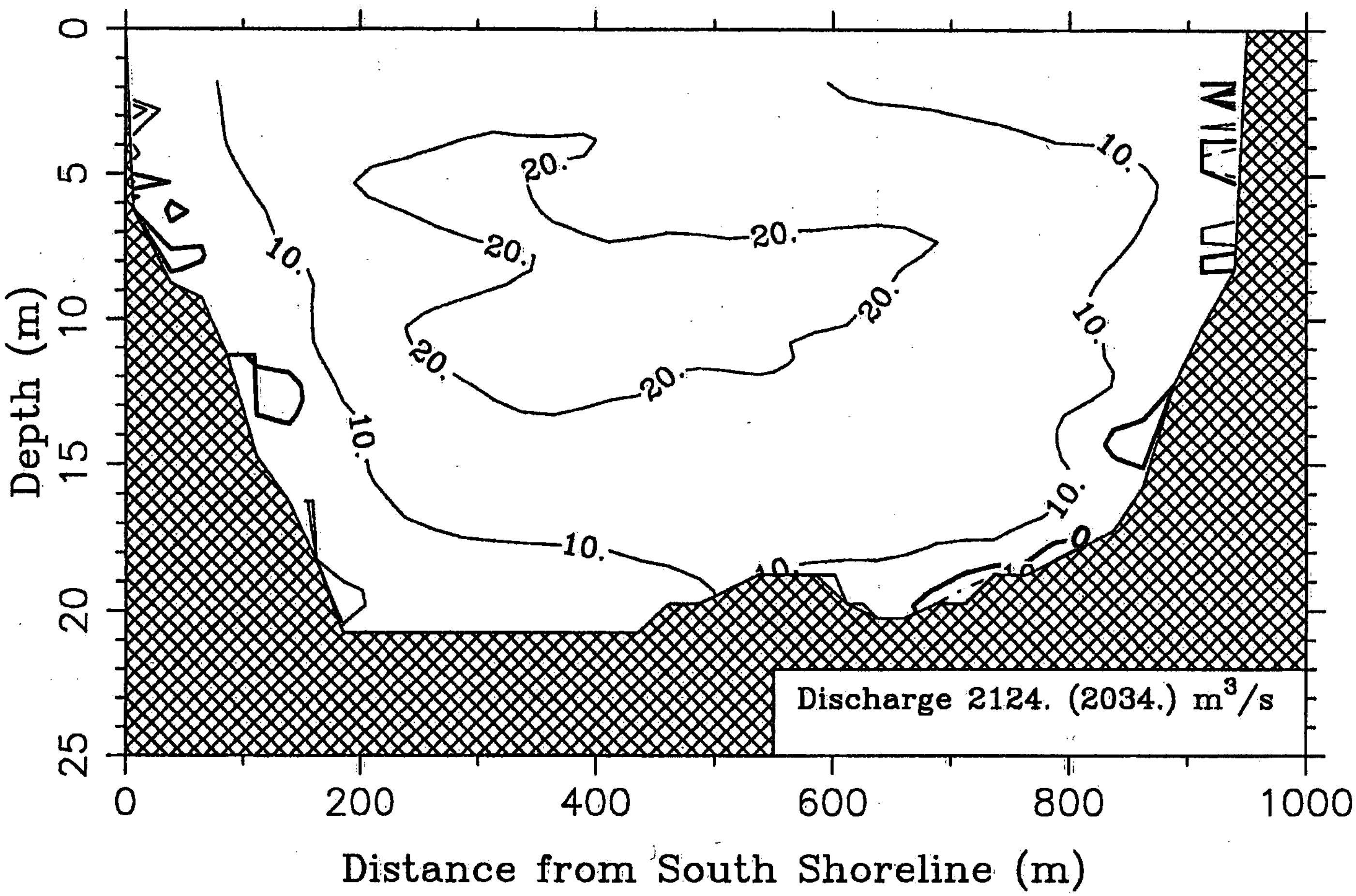

Figure 8b

South Downstream Flow (cm/s), August 22 19:44 to 20:52 North

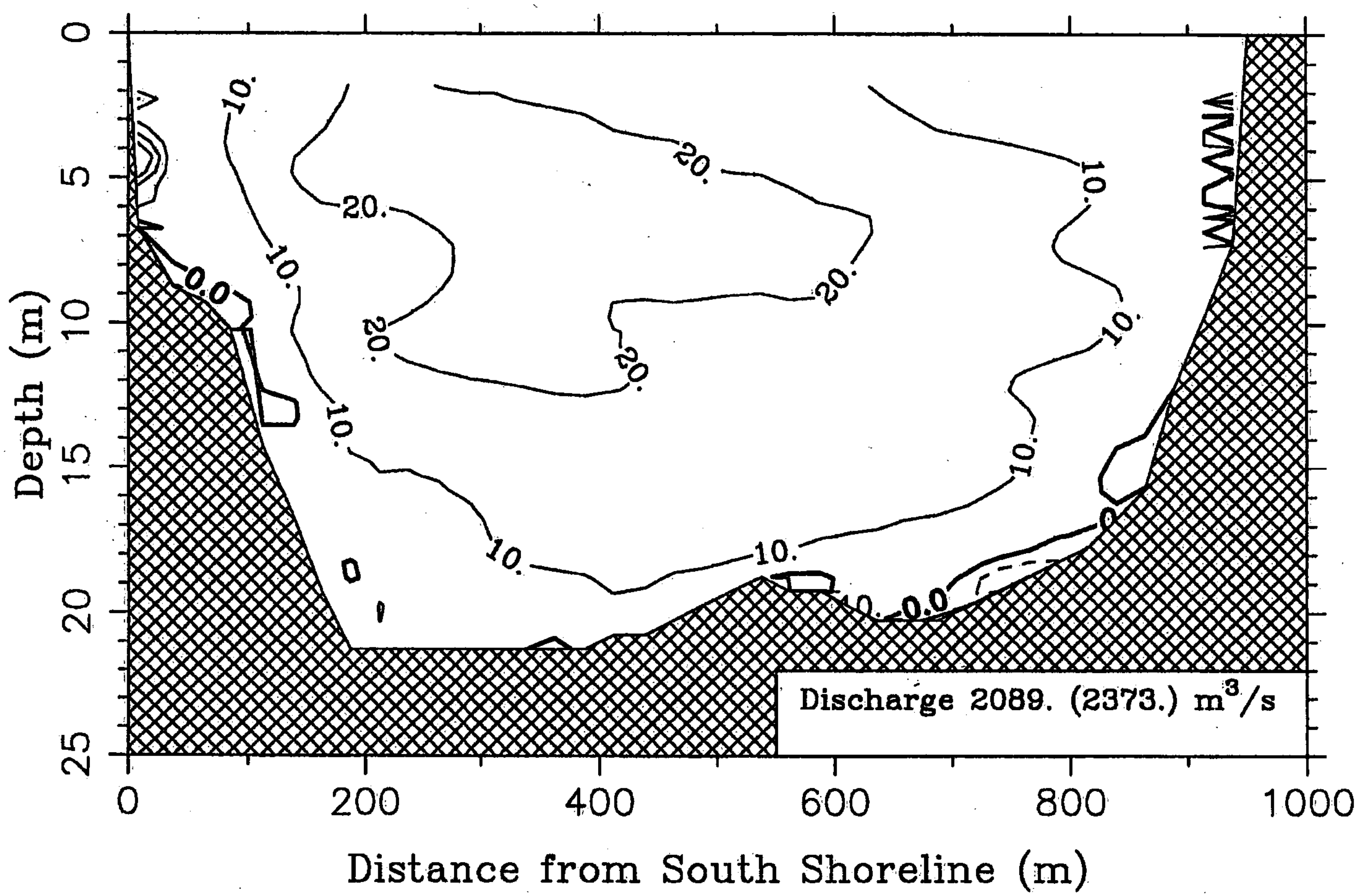

Figure 8c

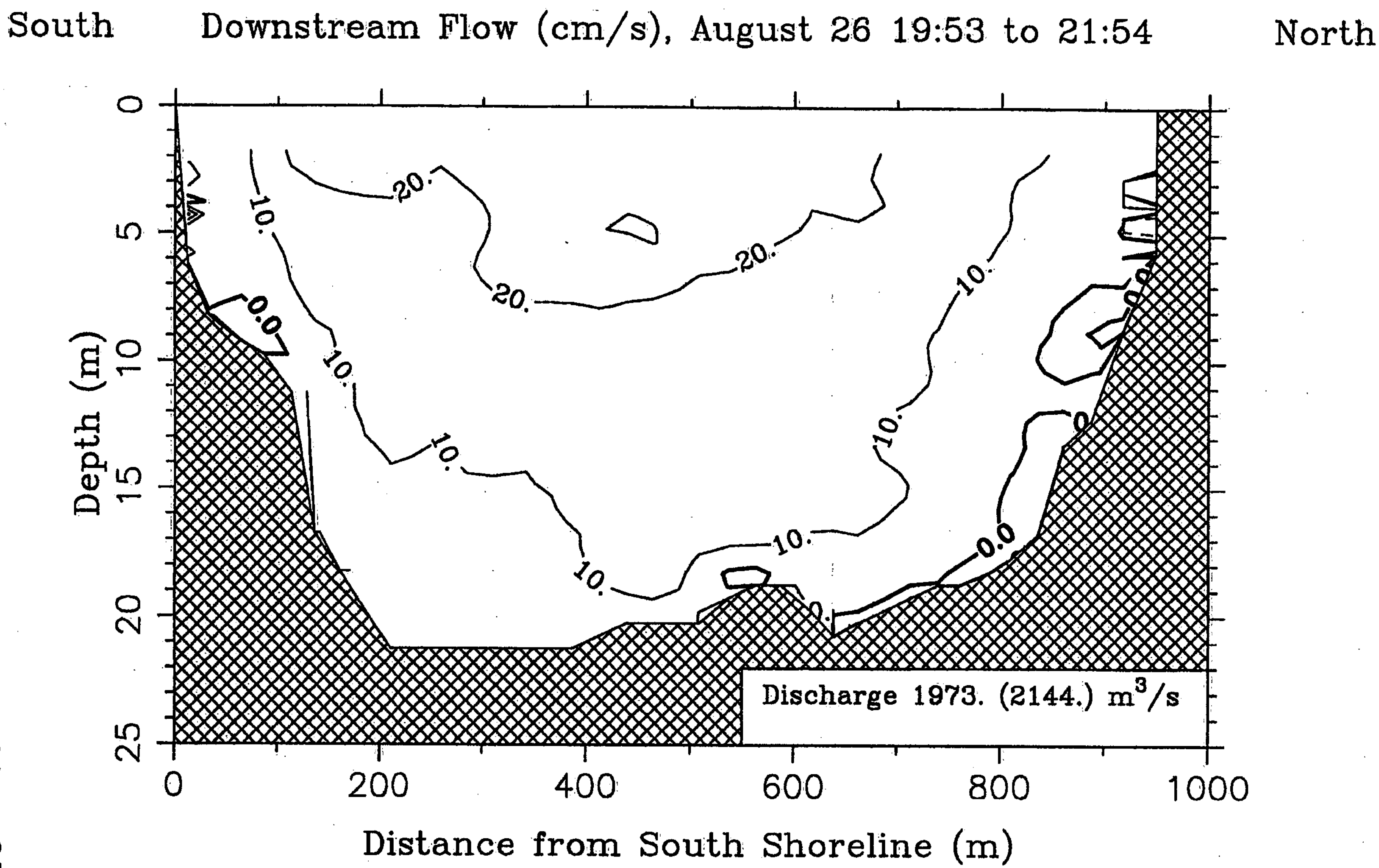

South
Downstream Flow (cm/s), August 26 19:53 to 21:54
North
Depth (m)
0
5
10
15
20
25
20.
20.
20.
10.
10.
10.
10.
10.
10.
10.
0.0
0.0
0.0
0
Discharge 1973. (2144.) m^3/s
0
200
400
600
800
1000
Distance from South Shoreline (m)

Figure 8d

South Downstream Flow (cm/s), August 28 00:38 to 00:56 North

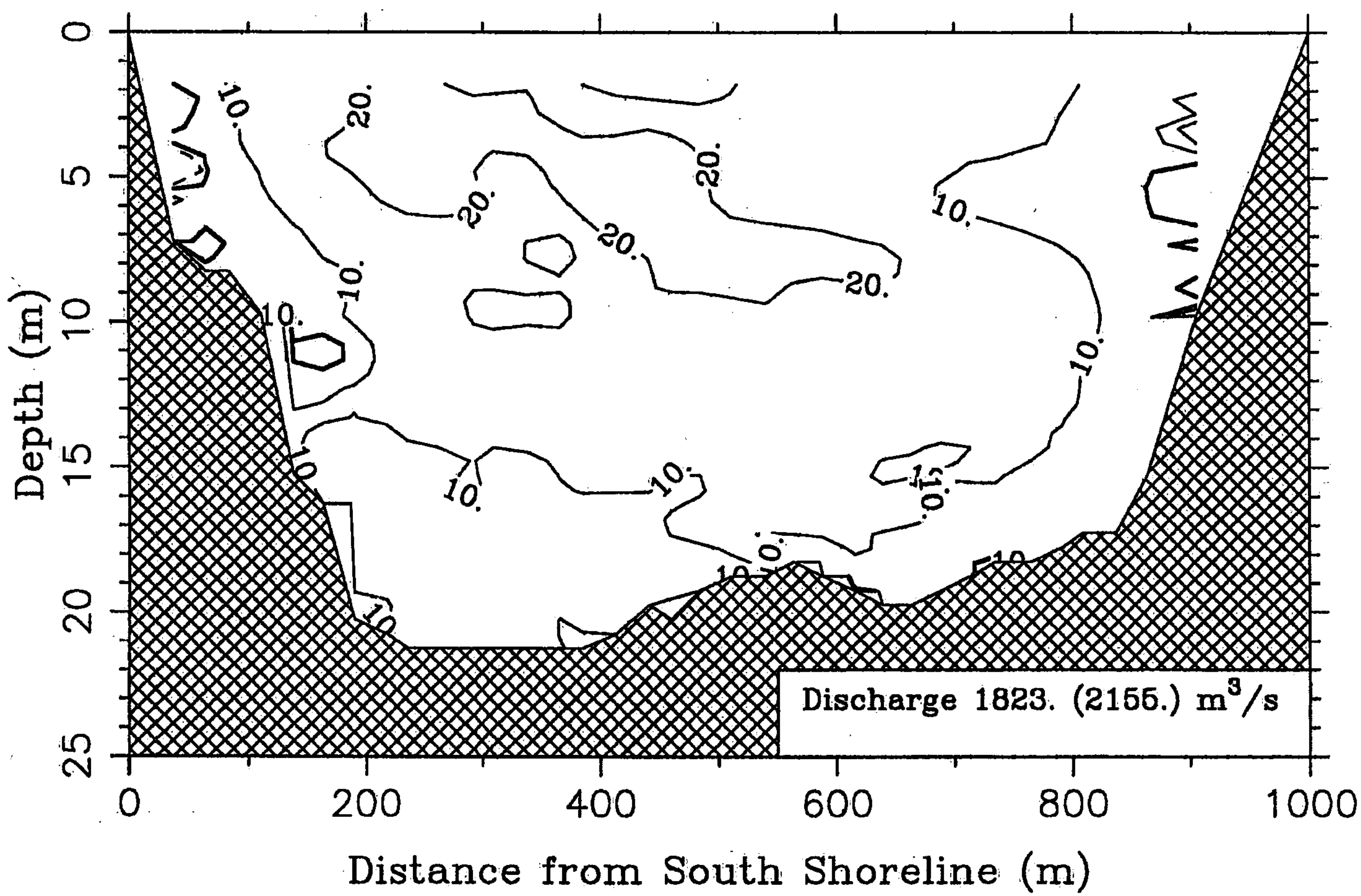

Figure 8e

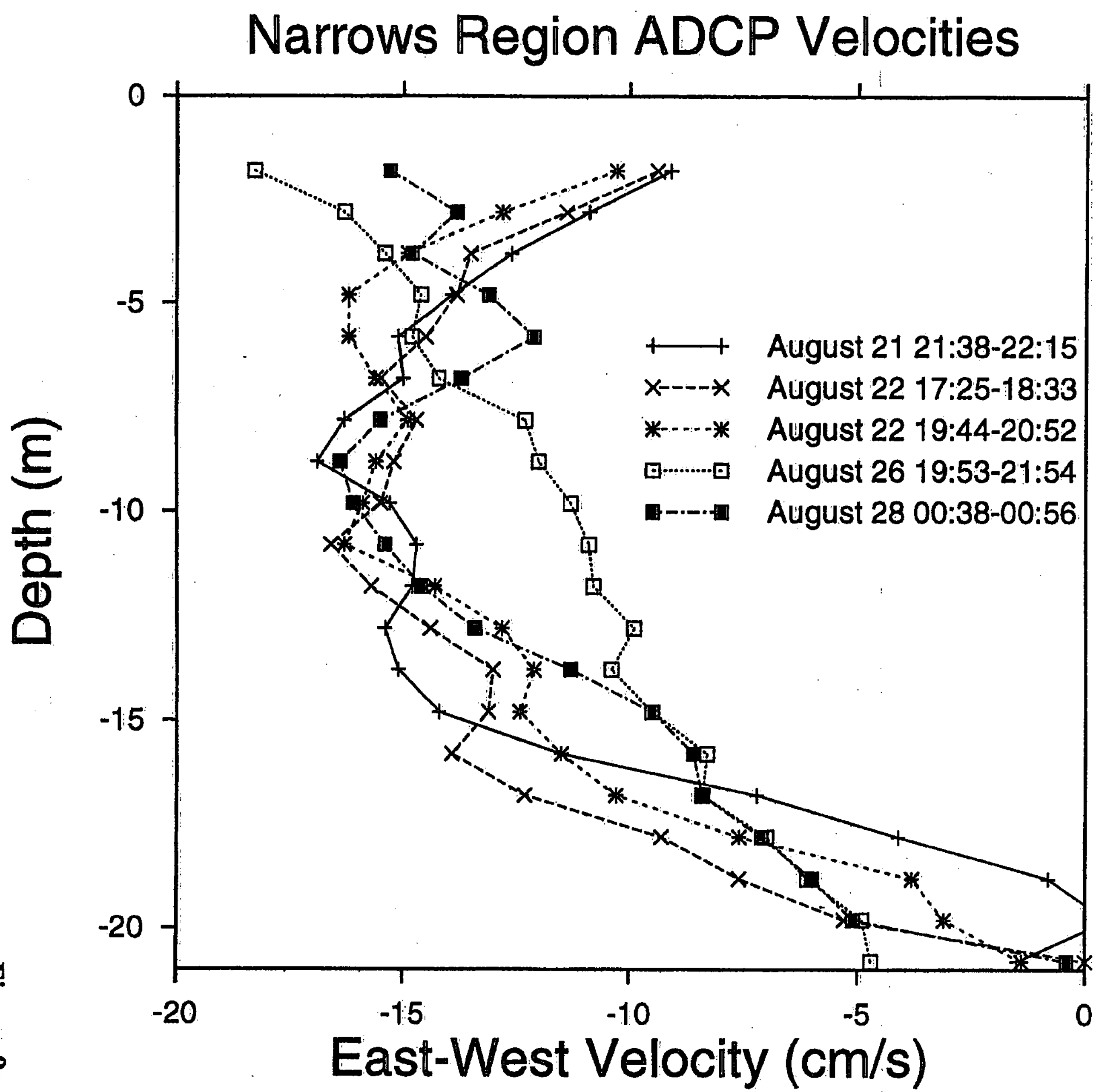
Narrows Region ADCP Velocities
0
-5
-10
-15
-20
Depth (m)
-20
-15
-10
-5
0
East-West Velocity (cm/s)
August 21 21:38-22:15
August 22 17:25-18:33
August 22 19:44-20:52
August 26 19:53-21:54
August 28 00:38-00:56

Figure 9a

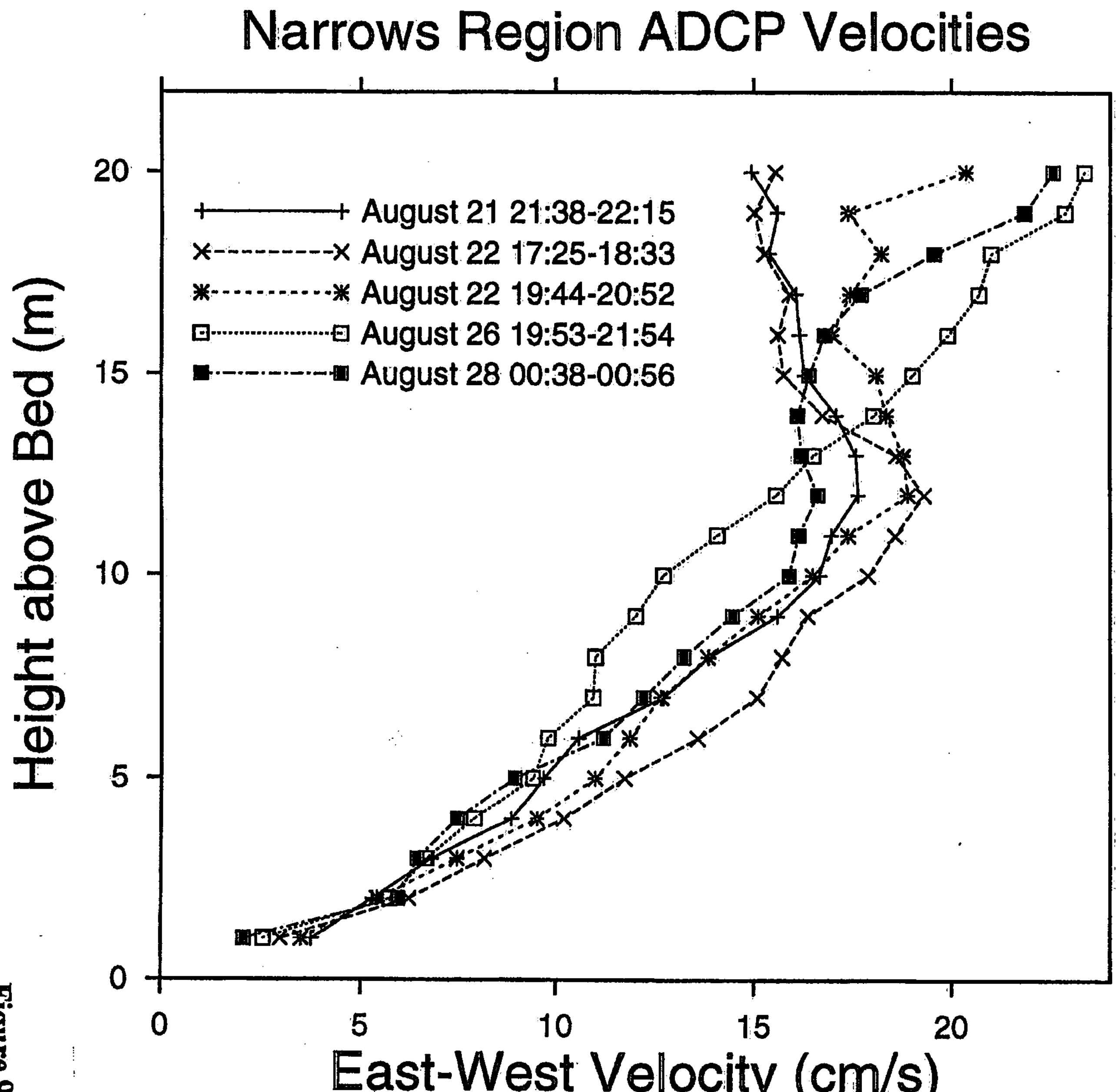

Narrows Region ADCP Velocities
Height above Bed (m)
East-West Velocity (cm/s)
August 21 21:38-22:15
August 22 17:25-18:33
August 22 19:44-20:52
August 26 19:53-21:54
August 28 00:38-00:56
0
5
10
15
20

Figure 9b

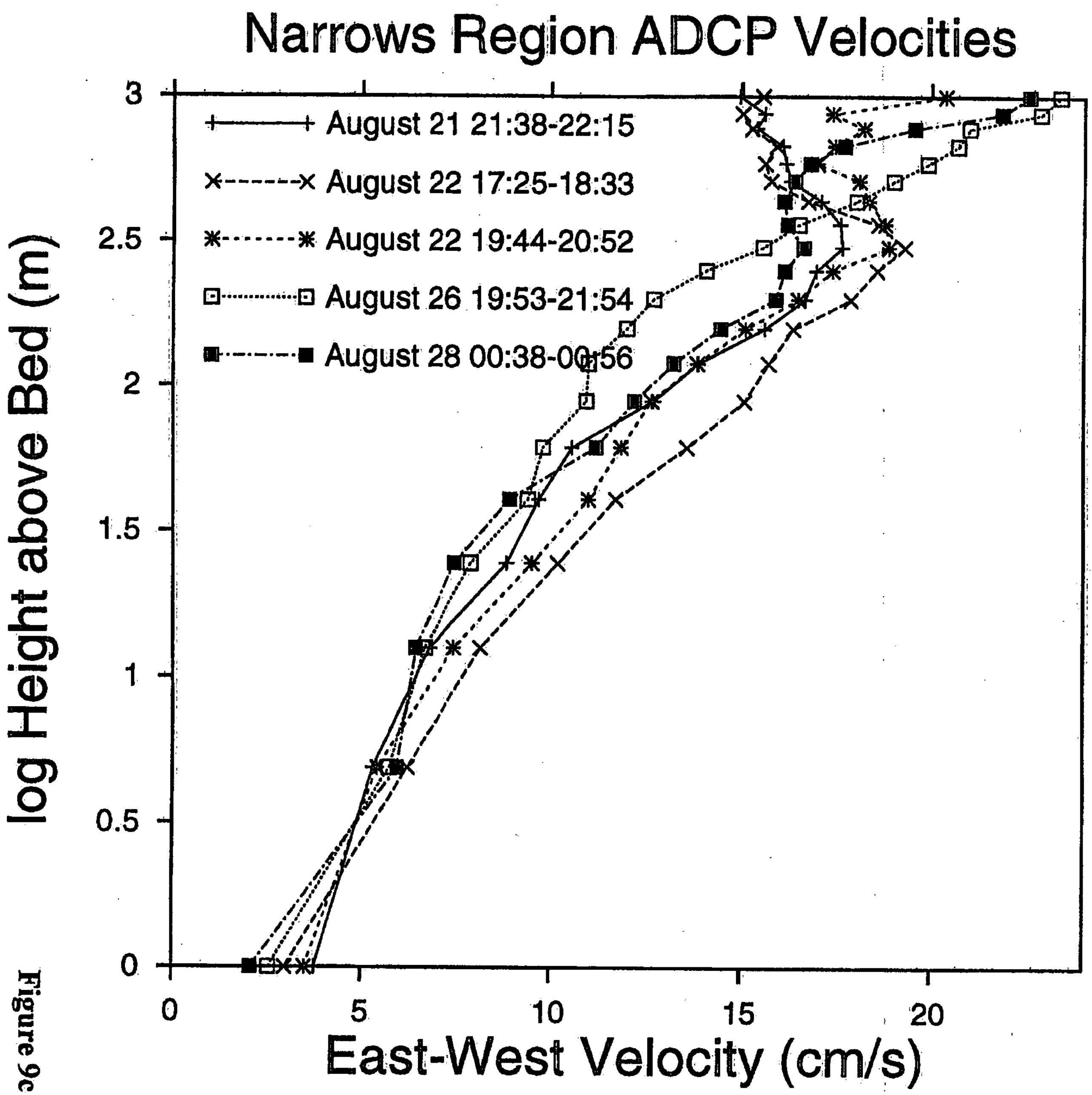

Narrows Region ADCP Velocities
log Height above Bed (m)
East-West Velocity (cm/s)
August 21 21:38-22:15
August 22 17:25-18:33
August 22 19:44-20:52
August 26 19:53-21:54
August 28 00:38-00:56
0
0.5
1
1.5
2
2.5
3
0
5
10
15
20

Figure 9c

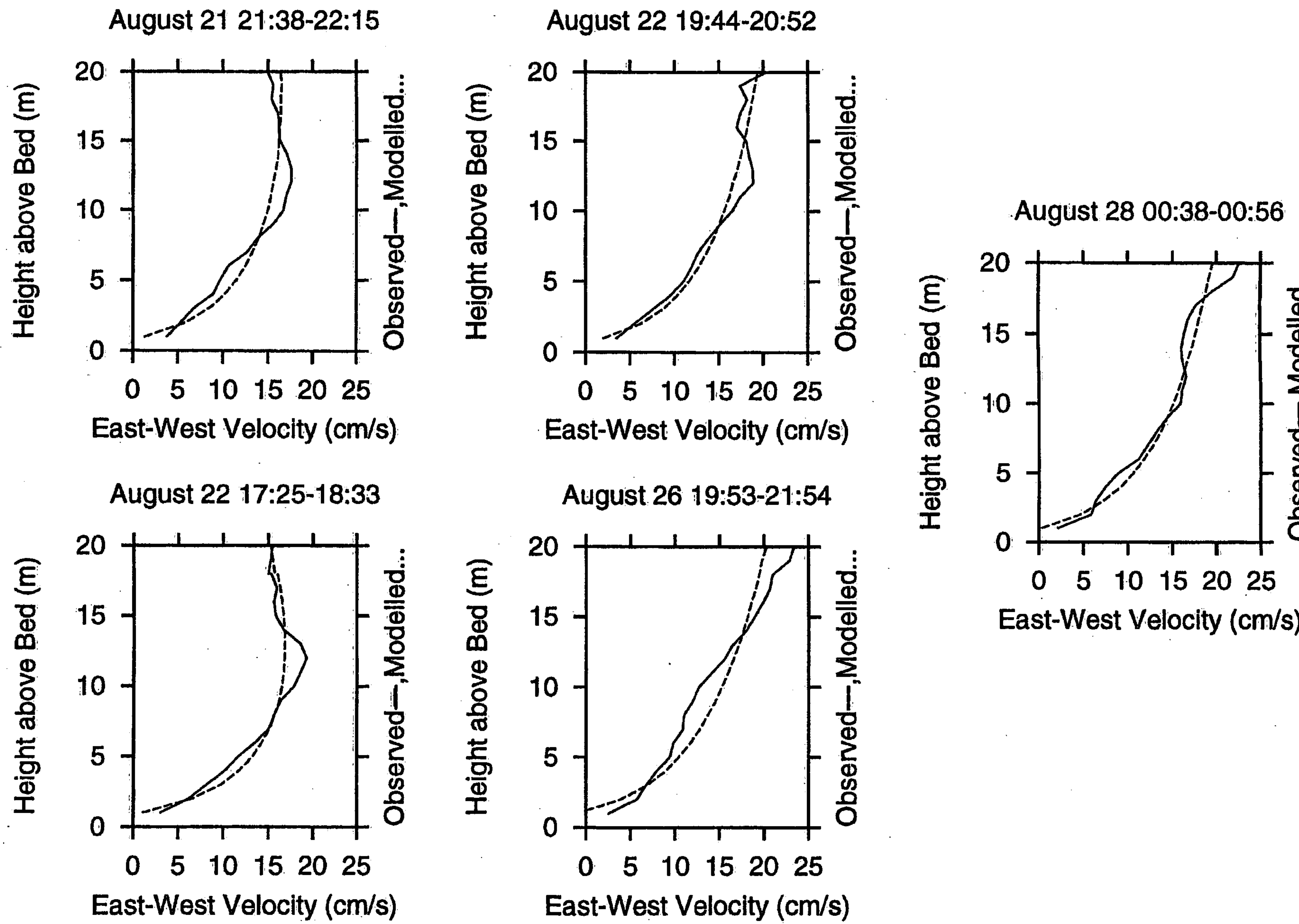
August 21 21:38-22:15
August 22 19:44-20:52
August 28 00:38-00:56
August 22 17:25-18:33
August 26 19:53-21:54
Height above Bed (m)
East-West Velocity (cm/s)
Observed—,Modelled...
0
5
10
15
20
25

FIGURE 10

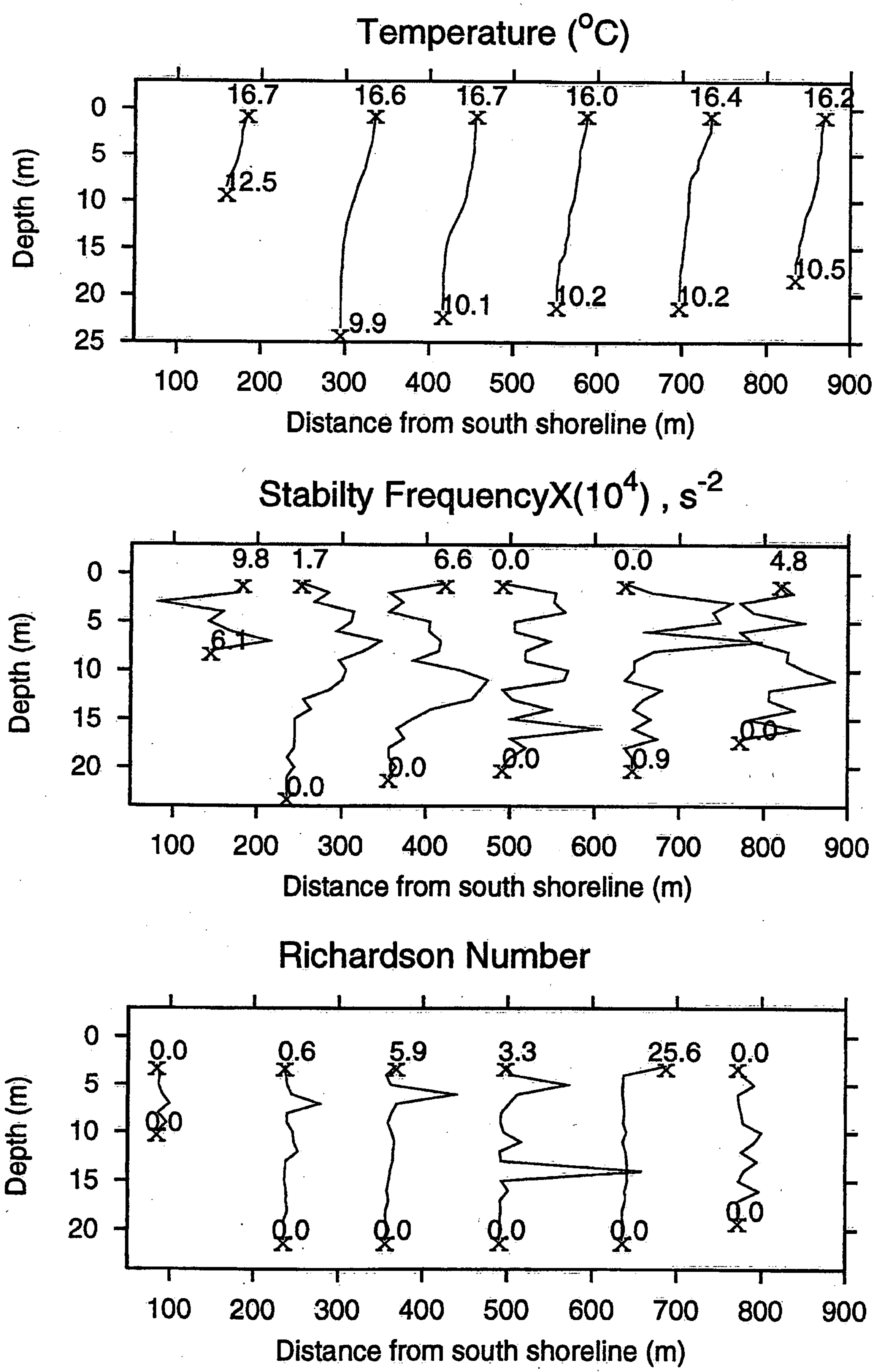

Temperature (°C)
Depth (m)
Distance from south shoreline (m)
16.7
16.6
16.7
16.0
16.4
16.2
12.5
9.9
10.1
10.2
10.2
10.5
Stabilty FrequencyX(10^4) , s^{-2}
9.8
1.7
6.6
0.0
0.0
4.8
6.1
0.0
0.0
0.0
0.9
0.0
Richardson Number
0.0
0.6
5.9
3.3
25.6
0.0
0.0
0.0
0.0
0.0
0.0
0.0

FIGURE 11

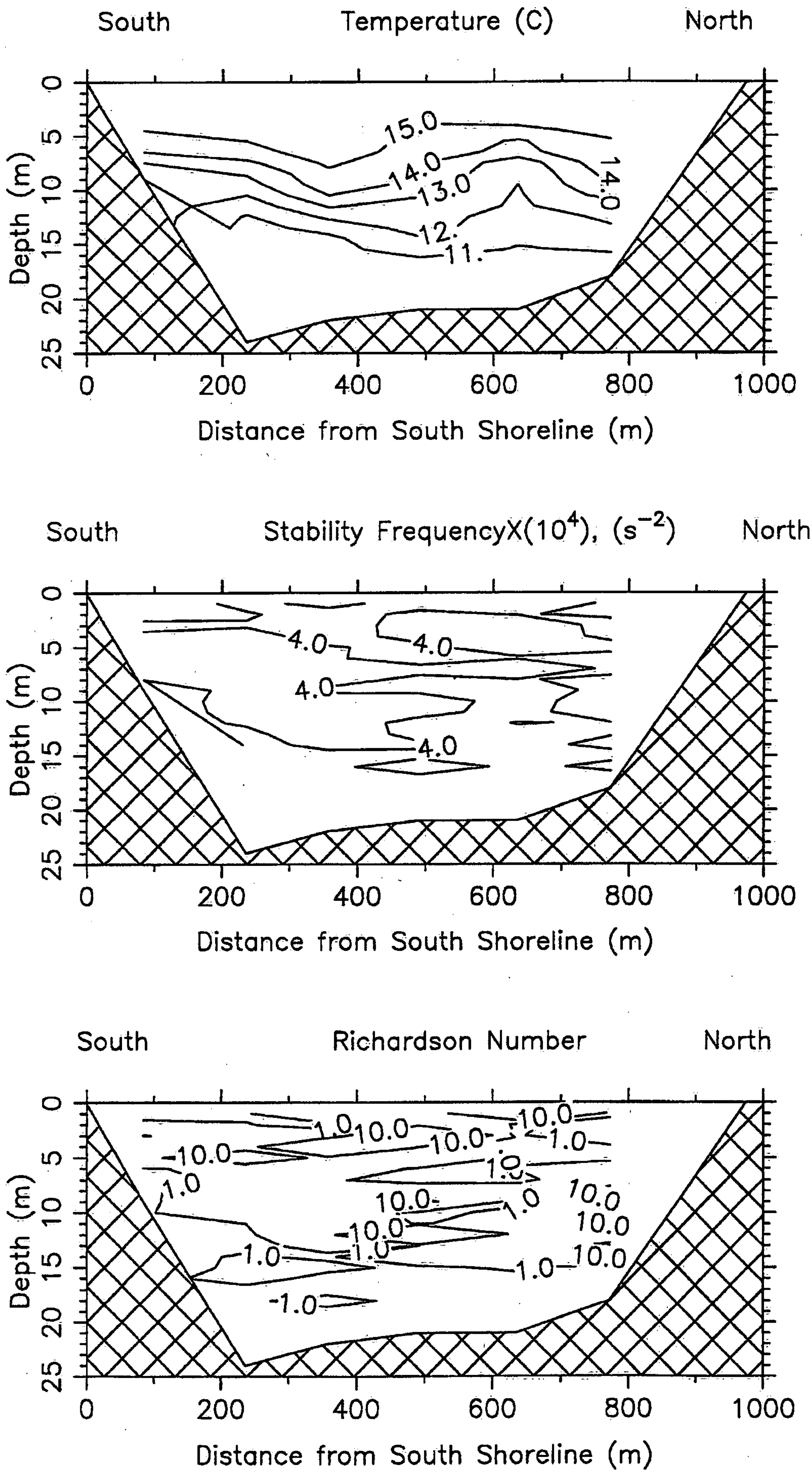
South
Temperature (C)
North
15.0
14.0
13.0
12.
11.
14.0
Depth (m)
Distance from South Shoreline (m)
South
Stability FrequencyX(10^4), (s^-2)
North
4.0
4.0
4.0
4.0
Depth (m)
Distance from South Shoreline (m)
South
Richardson Number
North
1.0
10.0
10.0
1.0
10.0
1.0
10.0
10.0
1.0
1.0
10.0
10.0
1.0
1.0
1.0
10.0
-1.0
Depth (m)
Distance from South Shoreline (m)

FIGURE 12

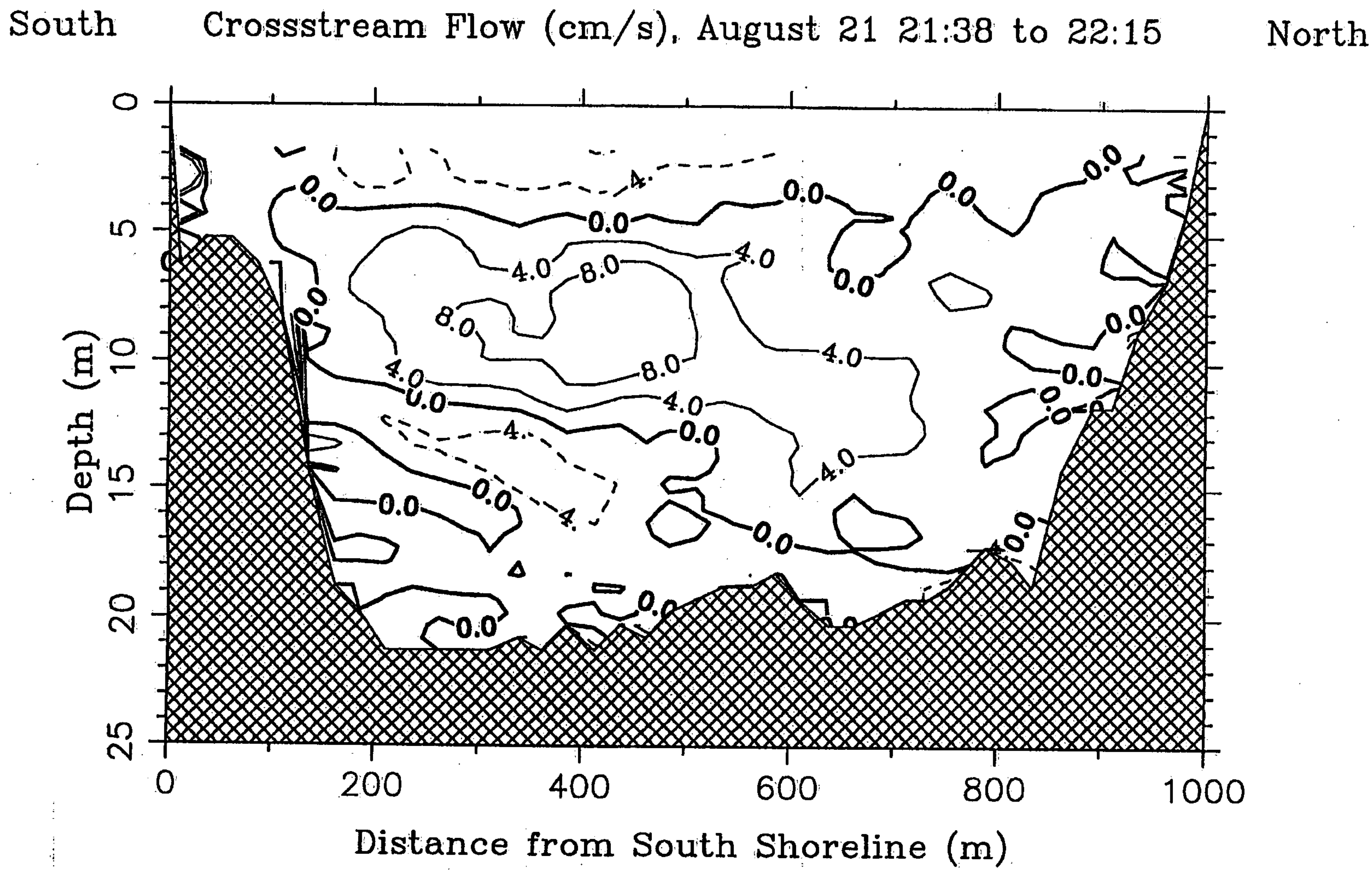
South
Crossstream Flow (cm/s), August 21 21:38 to 22:15
North
Depth (m)
Distance from South Shoreline (m)
0
5
10
15
20
25
0
200
400
600
800
1000
0.0
4.0
8.0
-4.

Figure 13a

South Cross Channel Flow (cm/s), August 22 17:25 to 18:33 North

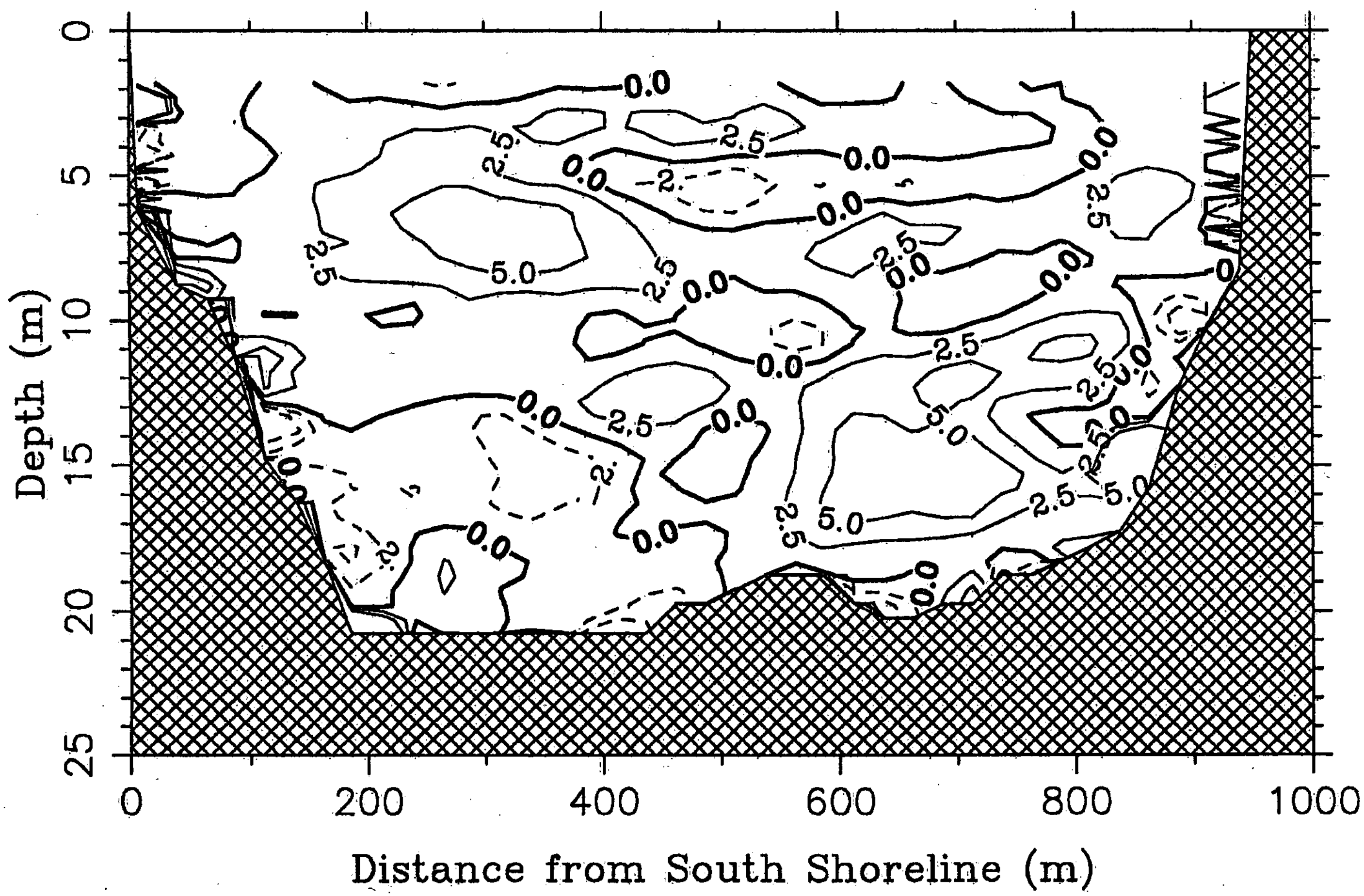

Figure 13b

South Cross Channel Flow (cm/s), August 22 19:44 to 20:52 North

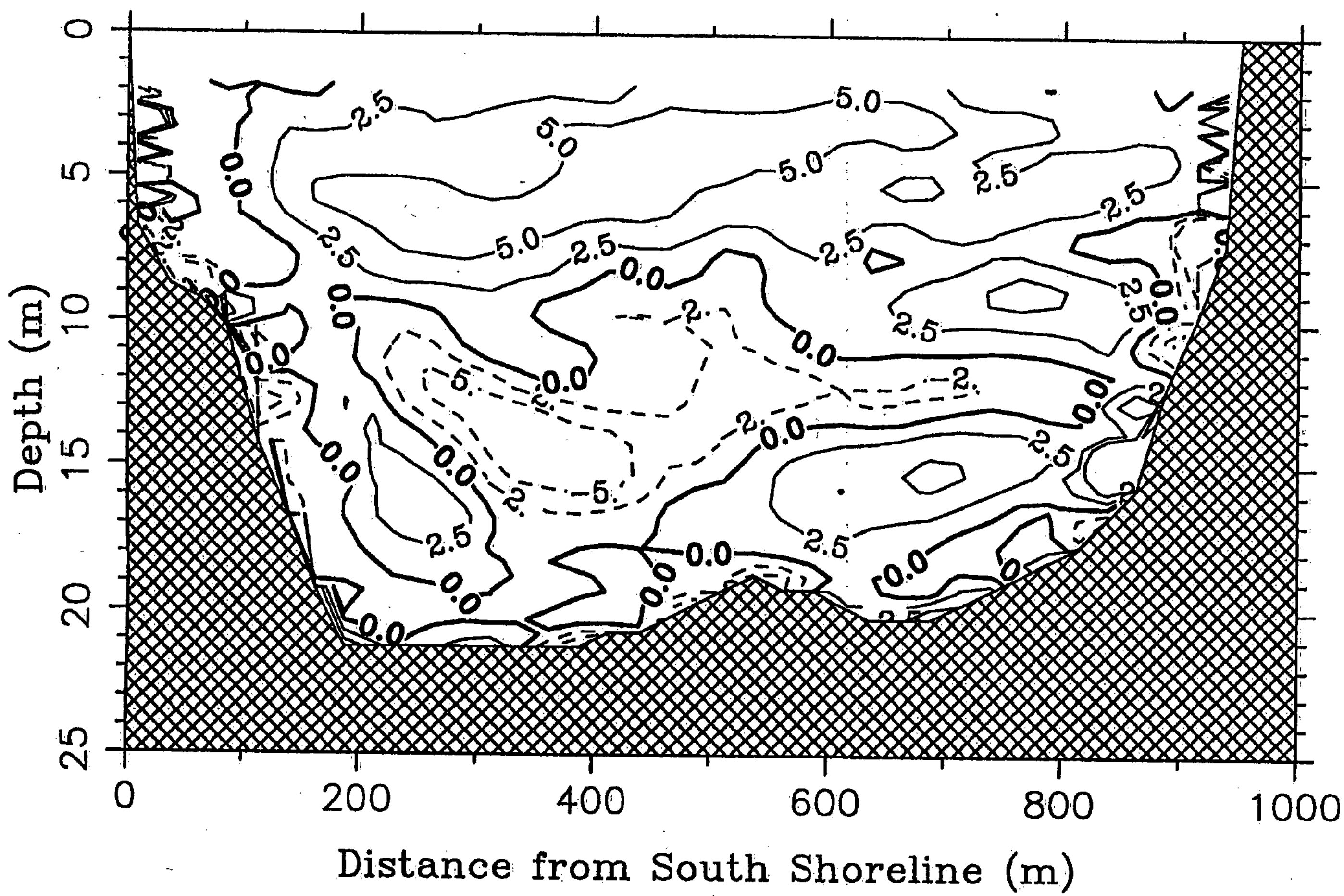

Figure 13c

South Cross Channel Flow (cm/s), August 26 19:53 to 21:20 North

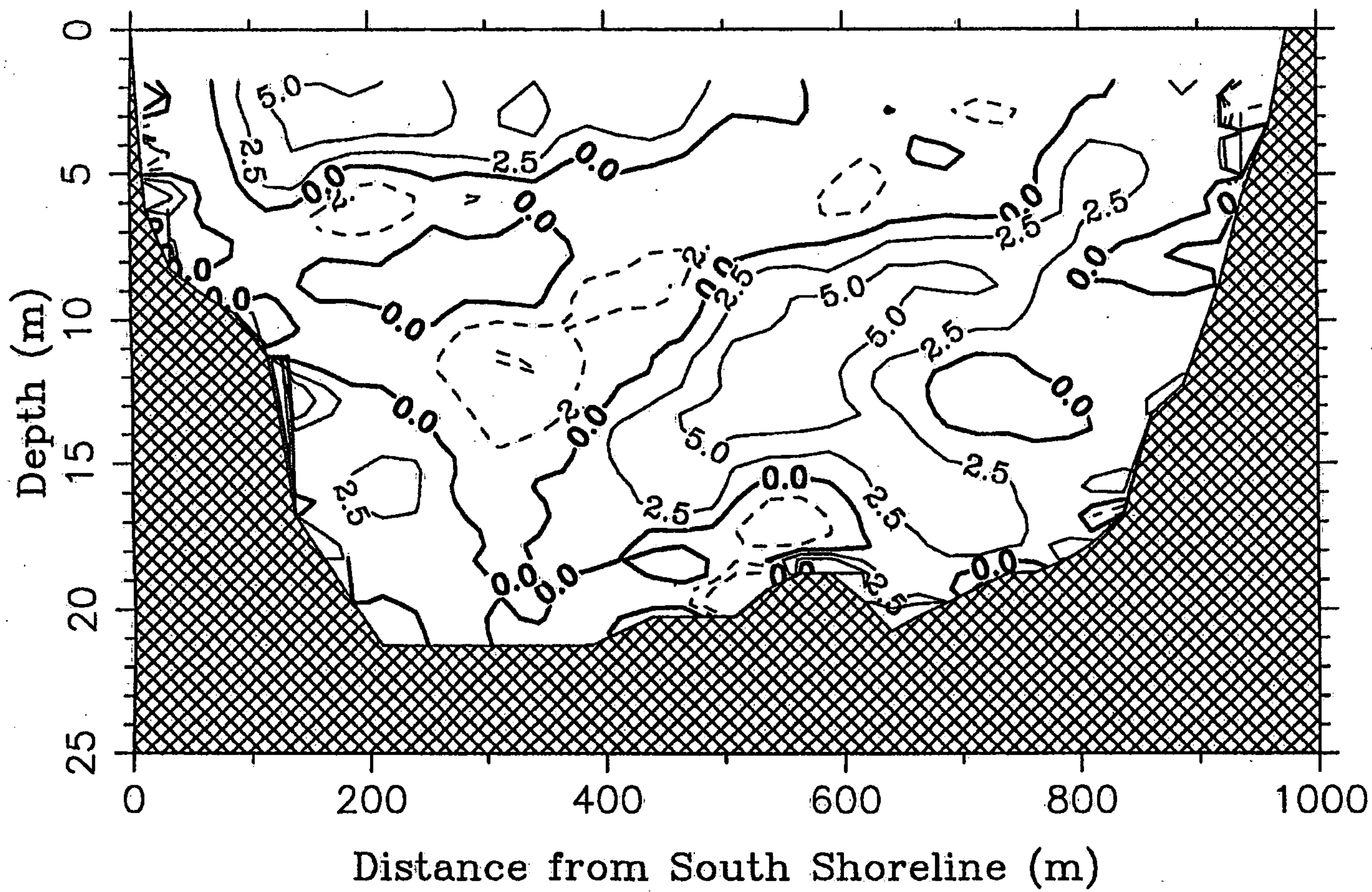

Figure 13d

South Cross Channel Flow (cm/s), August 28 00:38 to 00:56 North

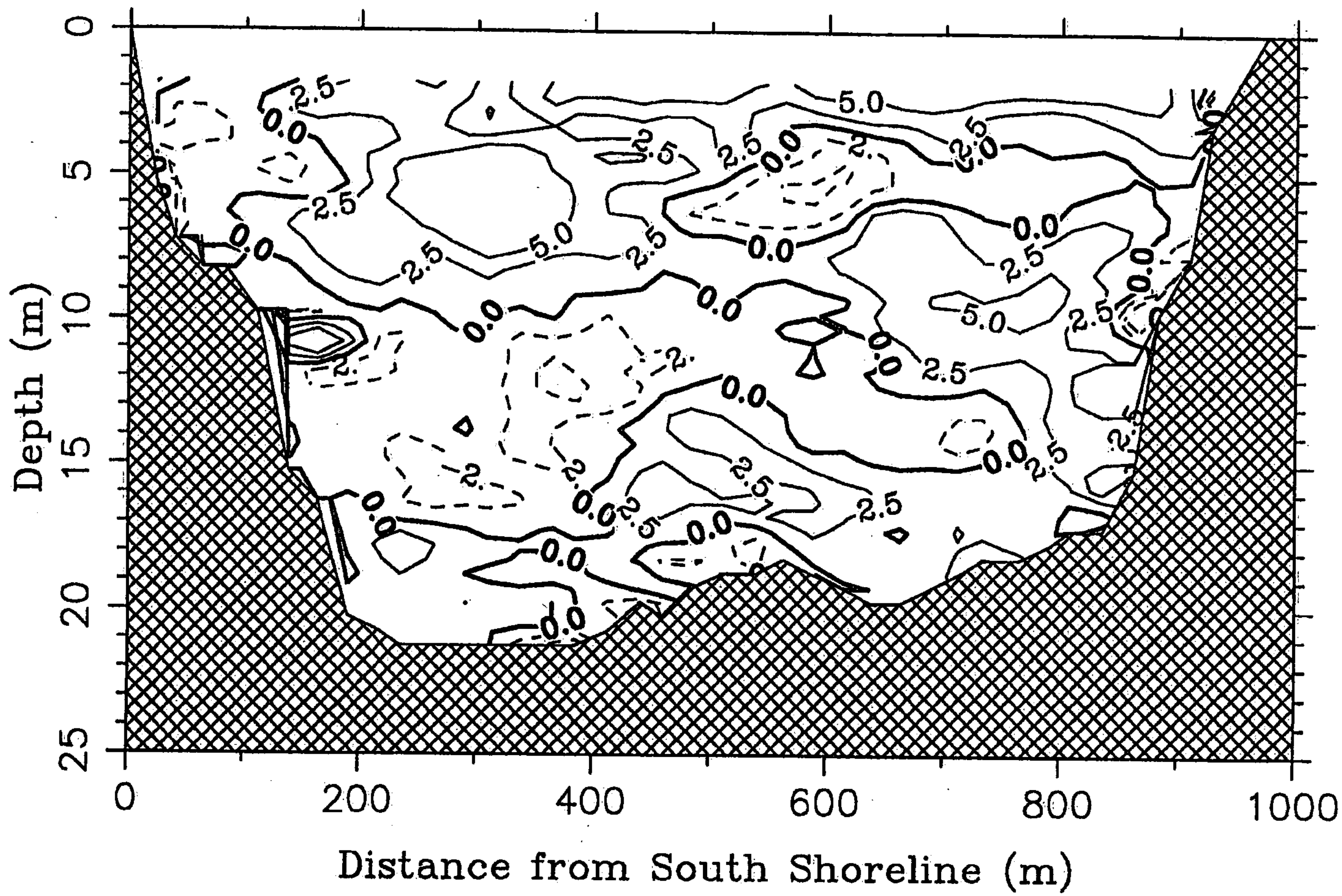

Figure 13e

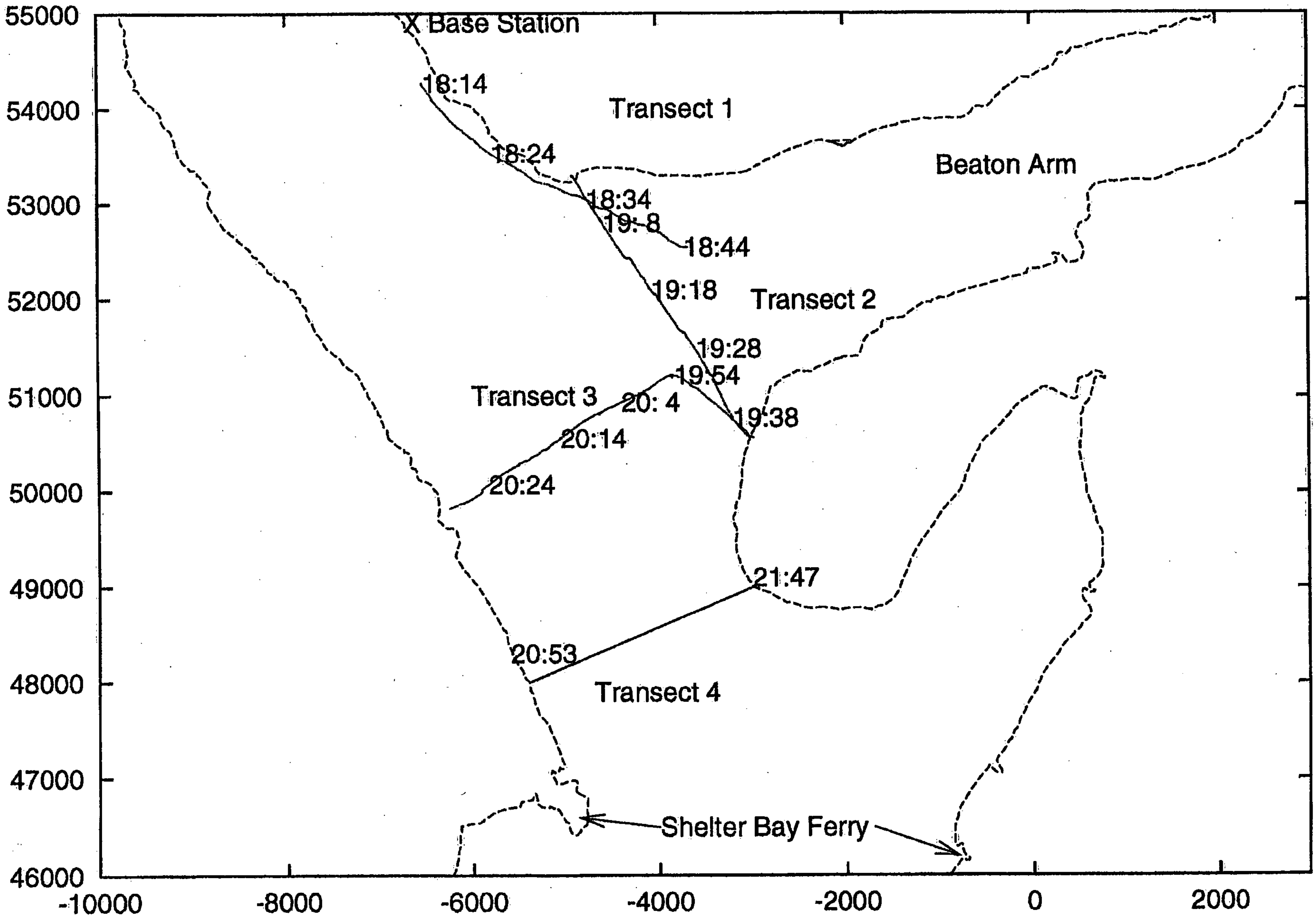
X Base Station
18:14
Transect 1
18:24
Beaton Arm
18:34
19: 8
18:44
19:18
Transect 2
19:28
19:54
Transect 3
20: 4
19:38
20:14
20:24
21:47
20:53
Transect 4
Shelter Bay Ferry
55000
54000
53000
52000
51000
50000
49000
48000
47000
46000
-10000
-8000
-6000
-4000
-2000
0
2000

FIGURE 14

NW Temperature (C) Transect 1 Upper Arrow Lake, SE

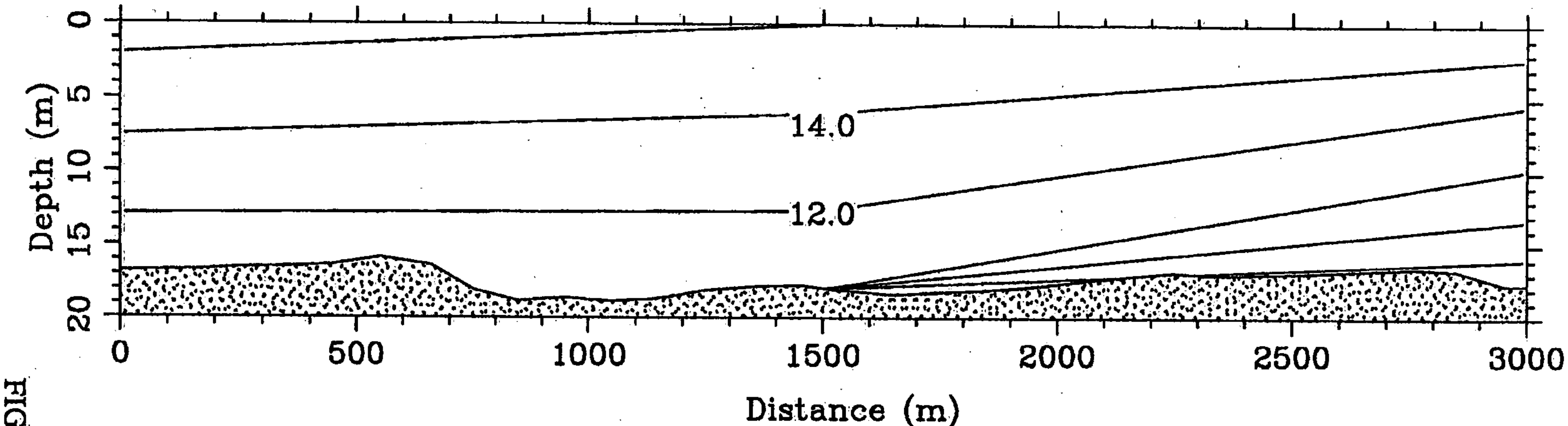

FIGURE 15

NW Flow along Transect 1 (cm/s) Upper Arrow Lake, SE

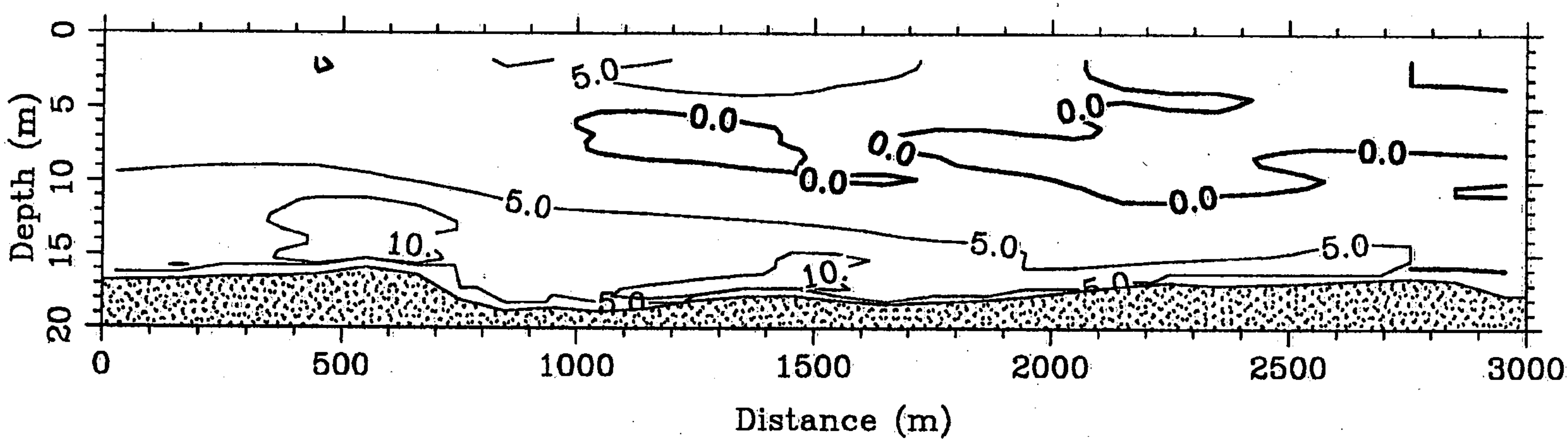

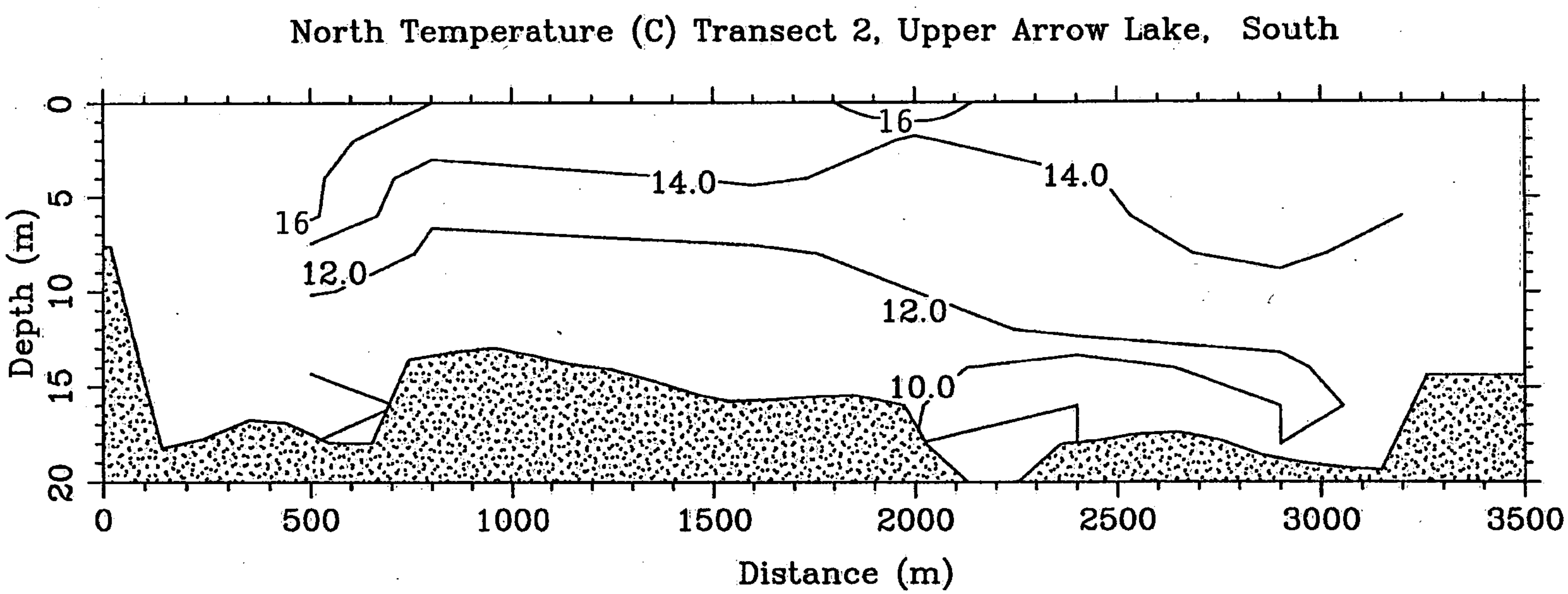
North Temperature (C) Transect 2, Upper Arrow Lake, South
16
14.0
14.0
16
12.0
12.0
10.0
Depth (m)
Distance (m)
0
500
1000
1500
2000
2500
3000
3500

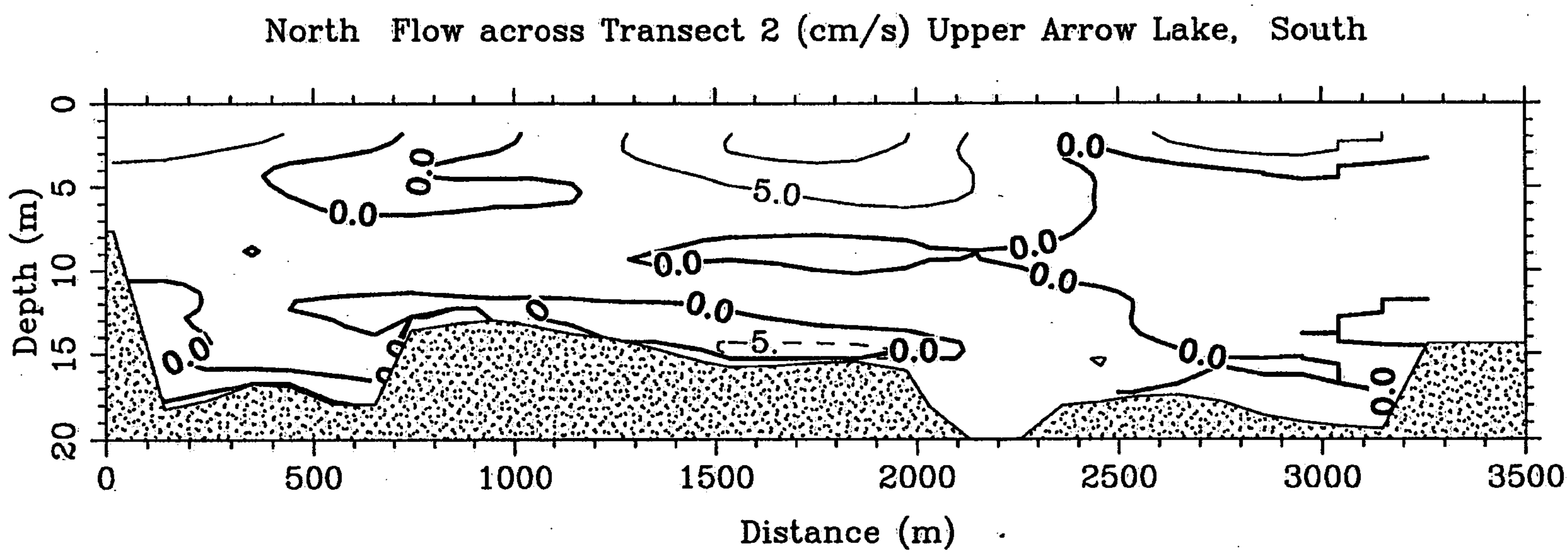
North Flow across Transect 2 (cm/s) Upper Arrow Lake, South
0.0
0.0
5.0
0.0
0.0
0.0
0.0
0.0
-5.
0.0
0.0
Depth (m)
Distance (m)
0
500
1000
1500
2000
2500
3000
3500

FIGURE 16

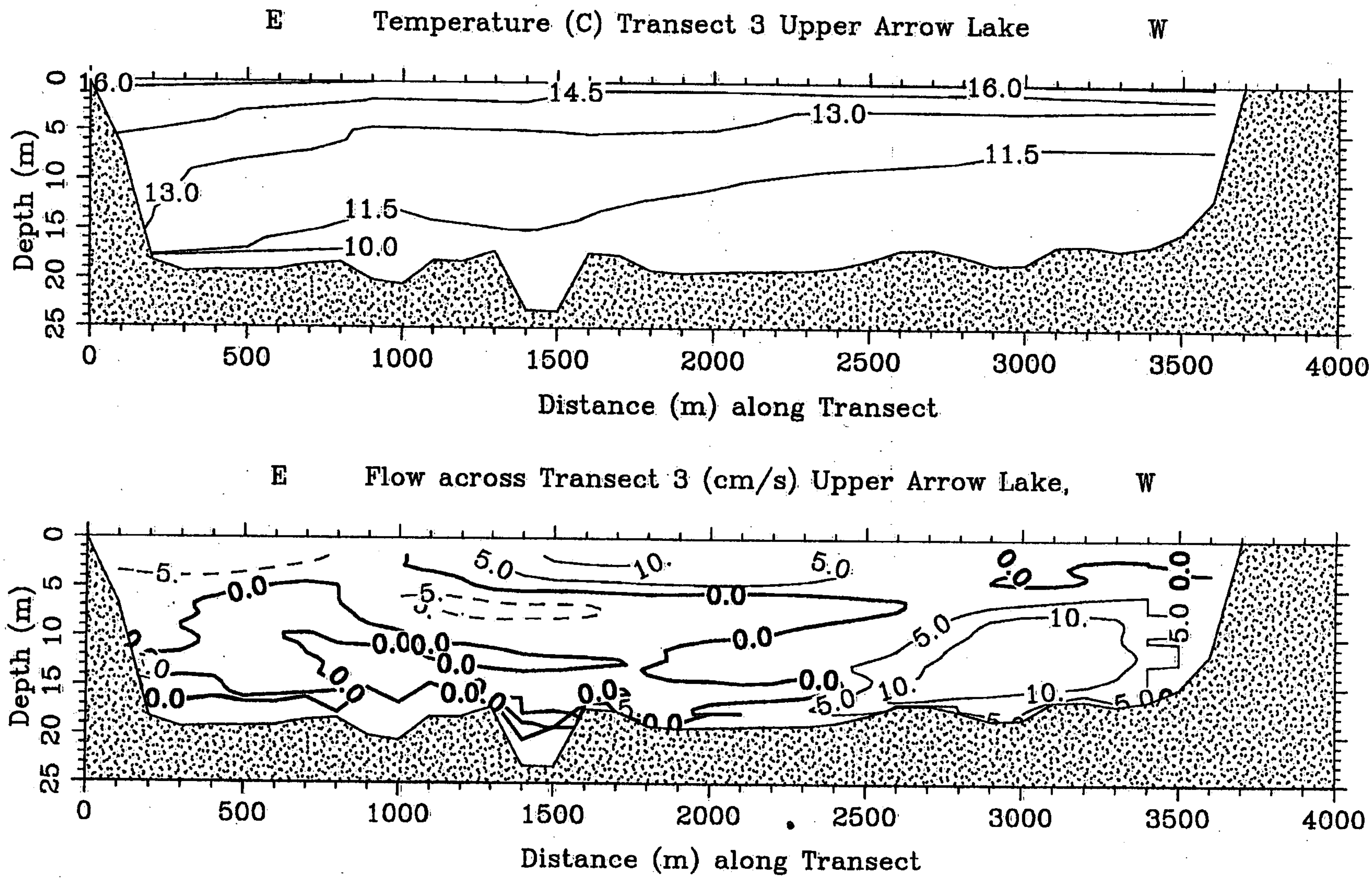
E
Temperature (C) Transect 3 Upper Arrow Lake
W
Depth (m)
Distance (m) along Transect
16.0
14.5
13.0
11.5
10.0
E
Flow across Transect 3 (cm/s) Upper Arrow Lake,
W
Depth (m)
Distance (m) along Transect
-5.
0.0
5.0
10.
-10.

FIGURE 17

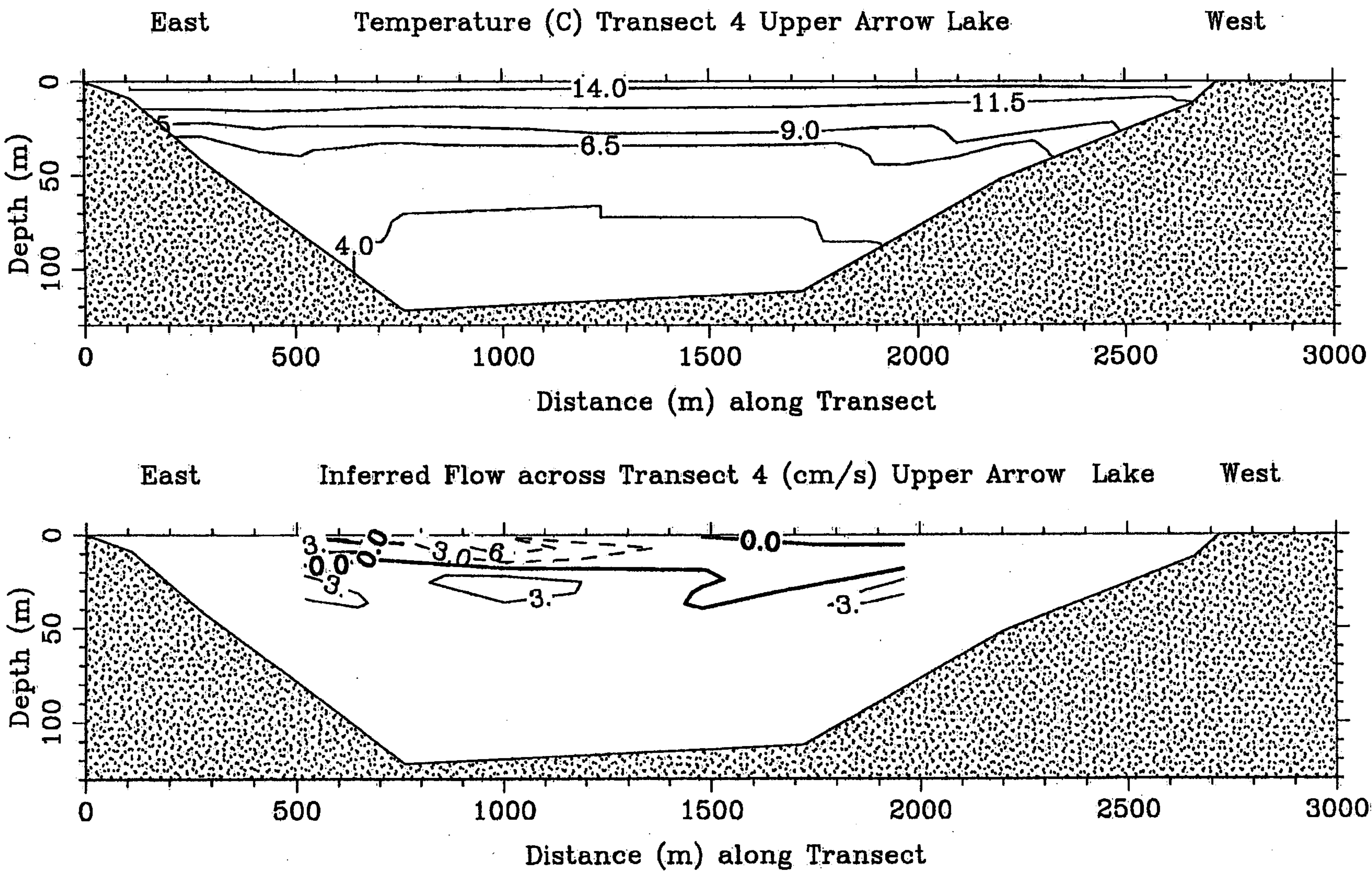
East
Temperature (C) Transect 4 Upper Arrow Lake
West
14.0
11.5
9.0
6.5
4.0
Depth (m)
0
50
100
0
500
1000
1500
2000
2500
3000
Distance (m) along Transect
East
Inferred Flow across Transect 4 (cm/s) Upper Arrow Lake
West
0.0
3.
-3.
Depth (m)
0
50
100
0
500
1000
1500
2000
2500
3000
Distance (m) along Transect

FIGURE 18

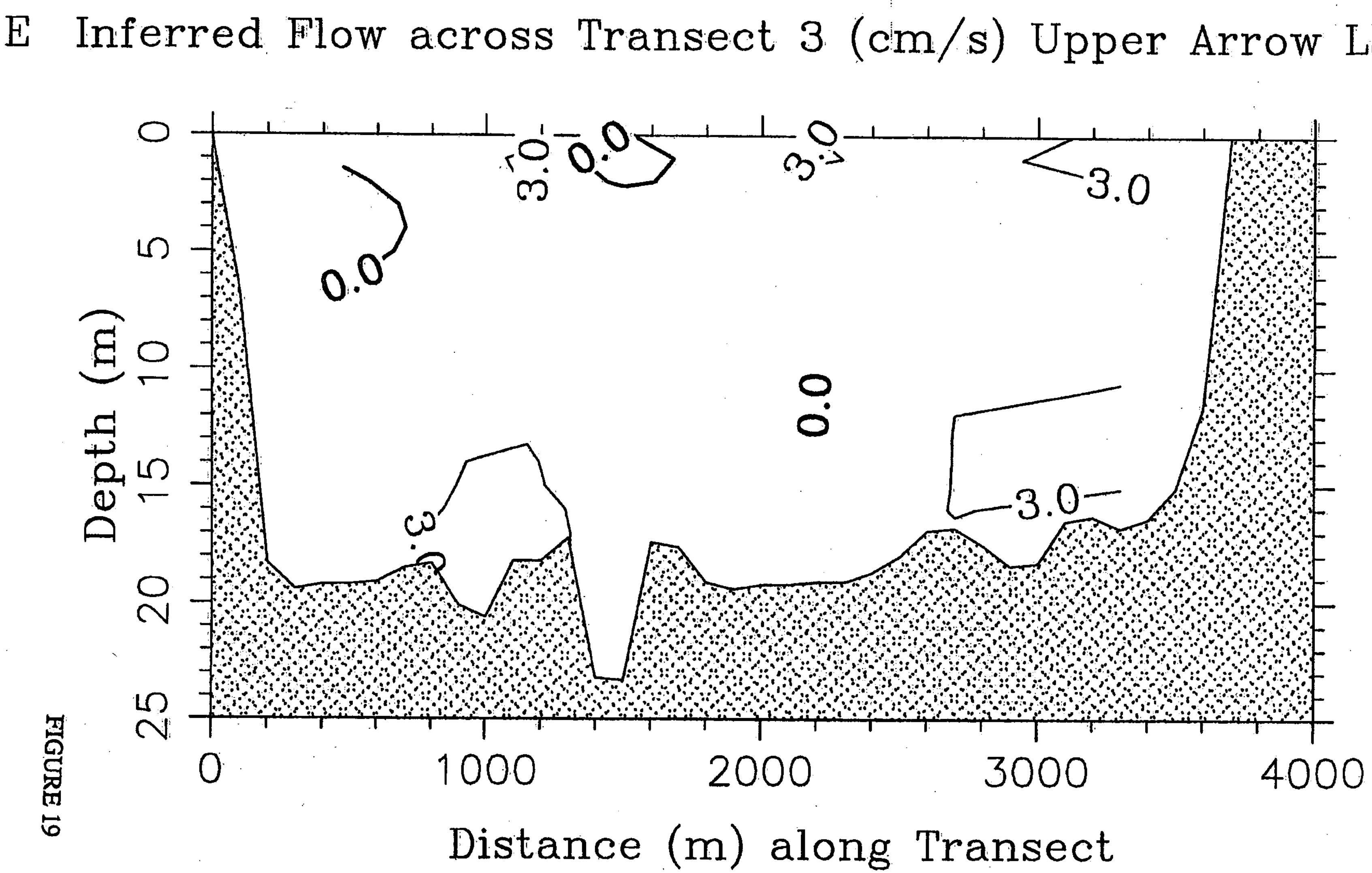
E Inferred Flow across Transect 3 (cm/s) Upper Arrow Lake W
Depth (m)
0
5
10
15
20
25
0.0
3.0
0
1000
2000
3000
4000
Distance (m) along Transect

FIGURE 19

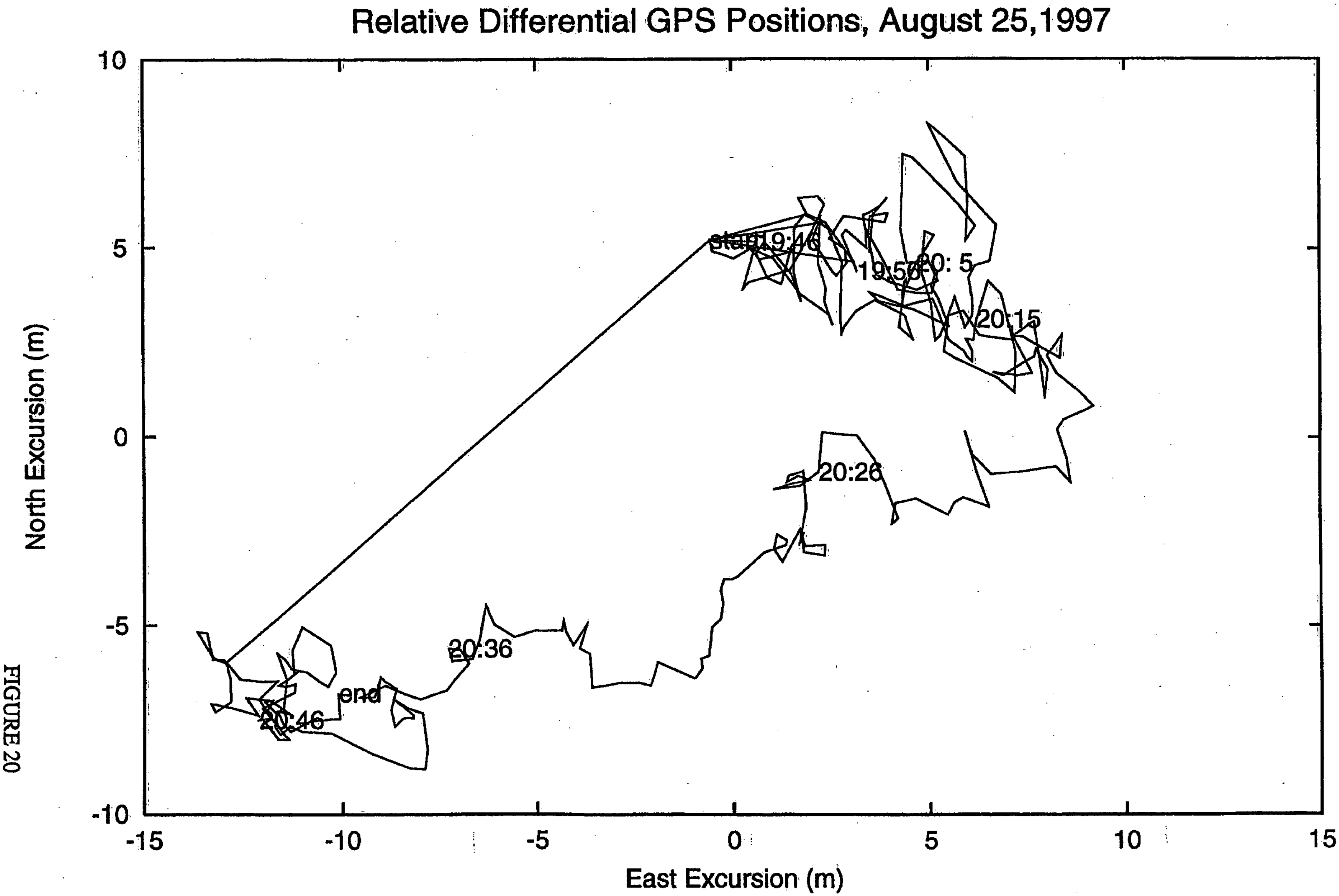

Relative Differential GPS Positions, August 25,1997
North Excursion (m)
East Excursion (m)
10
5
0
-5
-10
-15
-10
-5
0
5
10
15
start
19:46
19:56
20: 5
20:15
20:26
20:36
20:46
end

FIGURE 20

Velocity Profiles (cm/s) 1200 KHz ADCP, August 25, 1997

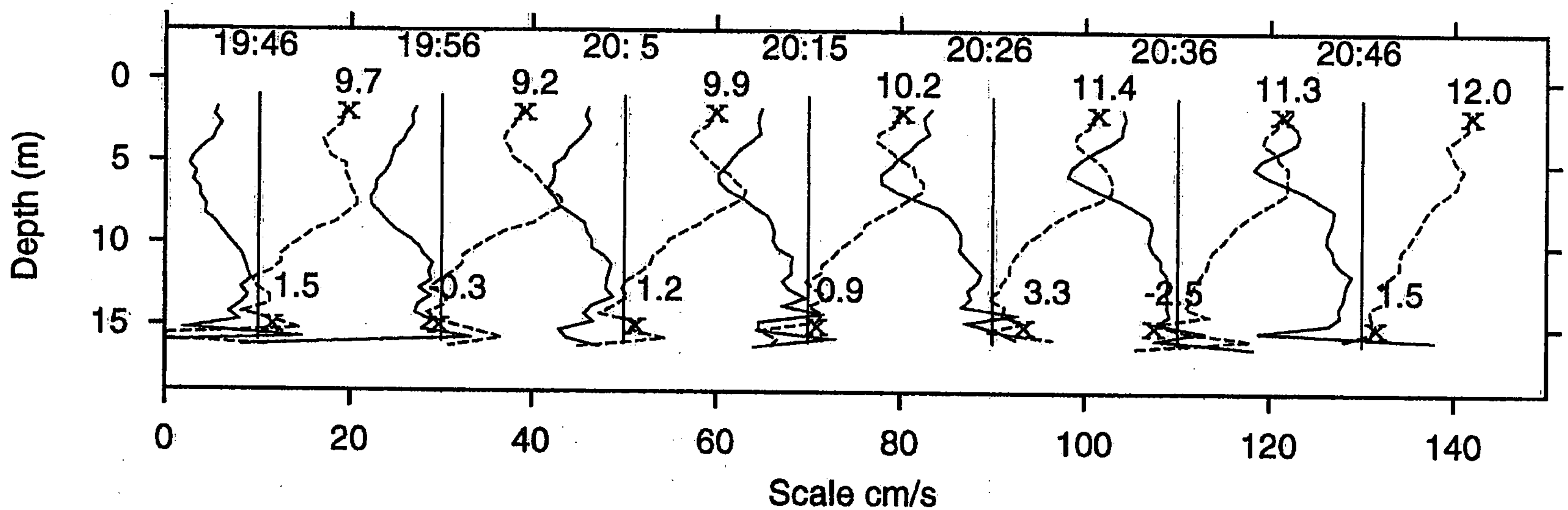

Velocity Profiles (cm/s) 300KHz ADCP, August 25, 1997

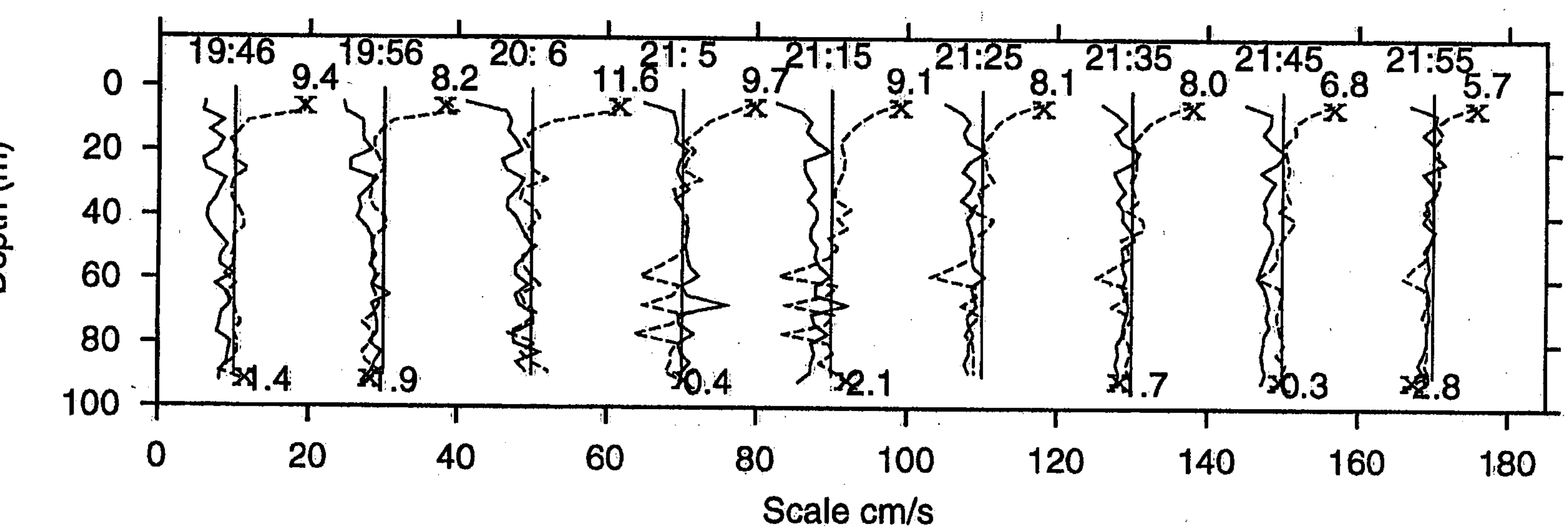

FIGURE 21

At Deep Hole

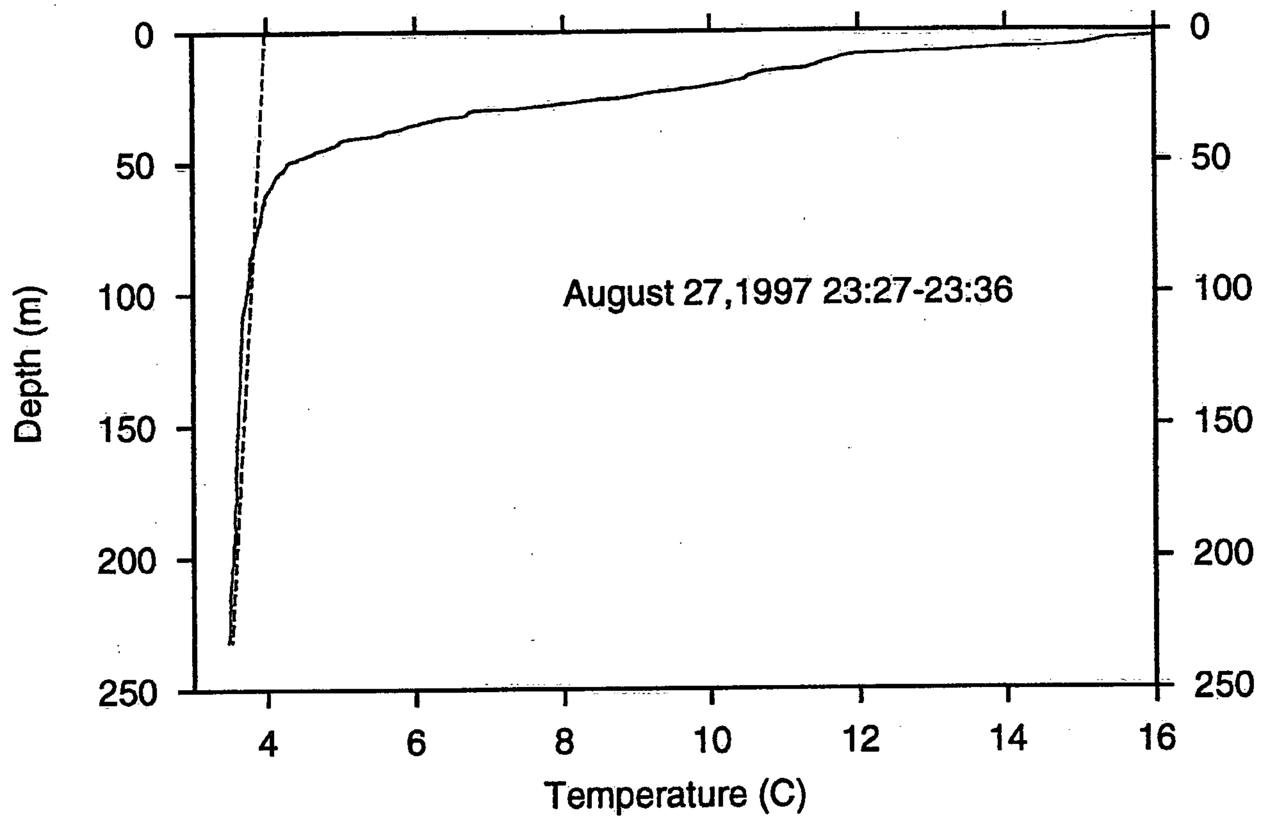

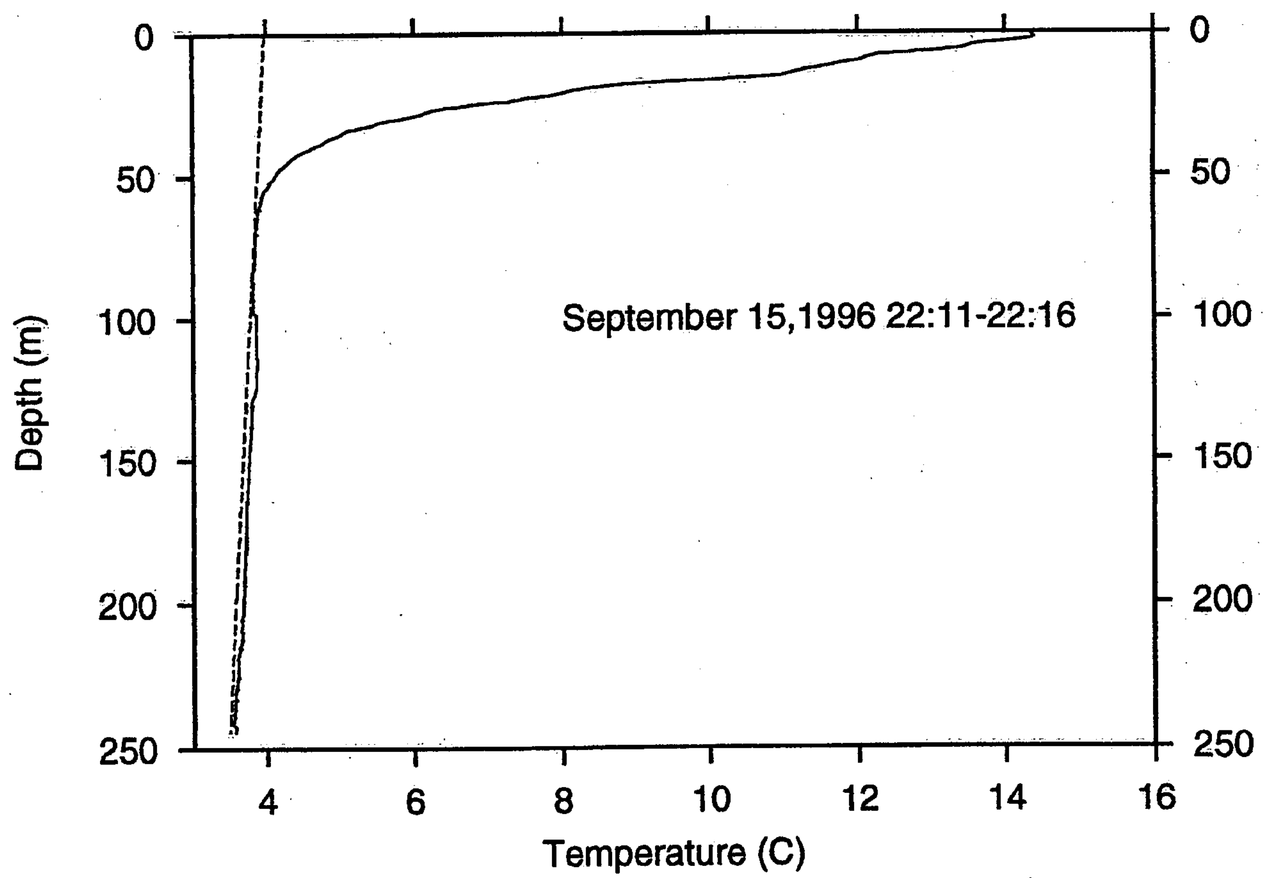

FIGURE 22

PRINTED IN CANADA ON RECYCLED PAPER
IMPRIMÉ AU CANADA SUR DU PAPIER RECYCLÉ

National Water Research Institute
Environment Canada
Canada Centre for Inland Waters
P.O. Box 5050
867 Lakeshore Road
Burlington, Ontario
L7R 4A6 Canada

National Hydrology Research Centre
11 Innovation Boulevard
Saskatoon, Saskatchewan
S7N 3H5 Canada

NATIONAL WATER RESEARCH INSTITUTE
INSTITUT NATIONAL DE RECHERCHE SUR LES EAUX

Institut national de recherche sur les eaux
Environnement Canada
Centre canadien des eaux intérieures
Case postale 5050
867, chemin Lakeshore
Burlington, Ontario
L7R 4A6 Canada

Centre national de recherche en hydrologie
11, boul. Innovation
Saskatoon, Saskatchewan
S7N 3H5 Canada

Environment Canada Environnement Canada

Canada